ANL-6907

ANL-6907

Argonne National Laboratory

THE EFFECT OF PARTICLE SIZE ON THE PROPERTIES OF GAS-FLUIDIZED BEDS

by

K. S. Sutherland

Printed in USA. Price $3.00. Available from the Clearinghouse for Federal Scientific and Technical Information, National Bureau of Standards, U. S. Department of Commerce, Springfield, Virginia

ANL-6907
Chemistry
(TID-4500, 34th Ed.)
AEC Research and
Development Report

ARGONNE NATIONAL LABORATORY
9700 South Cass Avenue
Argonne, Illinois 60440

THE EFFECT OF PARTICLE SIZE ON THE PROPERTIES OF GAS-FLUIDIZED BEDS

by

K. S. Sutherland*

Chemical Engineering Division

July 1964

*Guest Scientist from Atomic Energy Research Establishment, Harwell, Didcot, Berks., England. Current address: Nuclear Chemical Plant Ltd., Chematom House, St. James Avenue, West Ealing, London W. 13, England.

Operated by The University of Chicago
under
Contract W-31-109-eng-38
with the
U. S. Atomic Energy Commission

TABLE OF CONTENTS

	Page
ABSTRACT	9
1. INTRODUCTION	9
2. THE EFFECT OF PARTICLE SIZE ON THE PROPERTIES OF FLUIDIZED BEDS	10
2.1 The Characteristics of Fluidization by Gases	10
2.2 The Effect of Particle Size on Bed Properties	11
3. QUALITY OF FLUIDIZATION	12
4. PRESSURE-DROP FLUCTUATIONS IN A FLUIDIZED BED	15
4.1 Previous Experimental Methods	15
4.2 The Effect of Gas Bubbles on Pressure-drop Readings	16
5. EXPERIMENTAL SYSTEM	17
5.1 Apparatus	17
5.2 Apparatus Calibration	20
5.2.1 Rotameters	20
5.2.2 Transducer Calibration	20
5.2.3 Recorder Characteristics	20
5.2.4 Bubble Generator Calibration	21
5.3 Fluidized-bed Materials	21
5.4 Experimental Method	22
5.5 Experimental Program	23
6. PRESENTATION AND DISCUSSION OF RESULTS	24
6.1 Treatment of Data	24
6.2 Measurements of Fluidization Quality	26
6.2.1 Effects of Particle Size and Bed Diameter	26
6.2.2 Effects of Particle Density	34
6.2.3 Effects of Bed Height and Probe Position	35
6.2.4 Effect of Particle-size Distribution	39
6.2.5 General Summary of Particle-size Effects	43

TABLE OF CONTENTS

		Page
6.3	Behavior of Injected Gas Bubbles	44
6.3.1	Generated Bubble Size	44
6.3.2	Effects of Bed-particle Size	46
7.	CONCLUSIONS	50
8.	ACKNOWLEDGMENTS	51
9.	REFERENCES	52

LIST OF FIGURES

No.	Title	Page
1.	Diagram of Apparatus	17
2.	Sketch of Probes	18
3.	Electrical Circuits and Block Diagram	19
4.	Typical Fluidization Traces	24
5.	A Generalized Bubble Trace	26
6.	The Dependence of Minimum Fluidization Velocity on Average Bed-particle Size	27
7.	Trace Intensity versus Air Flow Rate for 60 Mesh Glass Beads, 3-in.-dia Column	28
8.	Trace Intensity versus Air Flow Rate for 80 Mesh Glass Beads, 5.5-in.-dia Column	29
9.	Trace Intensity versus Air Flow Rate for 60 Mesh Glass Beads, 11-in.-dia Column	29
10.	Intensity Measurements as a Function of Air Flow Rate for Various-sized Glass Beads, 3-in.-dia Column	30
11.	Intensity Measurements as a Function of Air Flow Rate for Various-sized Glass Beads, 5.5-in.-dia Column	30
12.	Intensity Measurements as a Function of Air Flow Rate for Various-sized Glass Beads, 11-in.-dia Column	31
13.	Intensity Measurements as a Function of Velocity Ratio for Various-sized Glass Beads, 3-in.-dia Column	31
14.	Intensity Measurements as a Function of Velocity Ratio for Various-sized Glass Beads, 5.5-in.-dia Column	32
15.	Intensity Measurements as a Function of Velocity Ratio for Various-sized Glass Beads, 11-in.-dia Column	32
16.	Intensity Measurements as a Function of Gas Velocity for Various-sized Glass Beads	33
17.	Intensity Measurements as a Function of Velocity for Materials of Different Densities	35
18.	Intensity Measurements as a Function of Velocity Ratio Showing Effect of Particle Size	36
19.	Intensity Measurements as a Function of Air Flow Rate Showing Effect of Probe Position	37

LIST OF FIGURES

No.	Title	Page
20.	Intensity Measurements as a Function of Air Flow Rate Showing Effect of Probe Separation	38
21.	Intensity Measurements as a Function of Air Flow Rate Showing Effect of Bed Height	38
22.	Intensity Measurements as a Function of Air Flow Rate Showing Effect of Particle Size Distribution for Addition of 120 Mesh to 60 Mesh Glass Beads	41
23.	Intensity Measurements as a Function of Air Flow Rate Showing Effect of Particle Size Distribution for Addition of 170 Mesh to 80 Mesh Glass Beads	41
24.	Intensity Measurements as a Function of Air Flow Rate Showing Effect of Particle Size Distribution for Addition of 120 Mesh to 170 Mesh Glass Beads	42
25.	Trace Length as a Function of Air Flow Rate Showing Effect of Particle Size Distribution for Mixture of 120 with 60 Mesh Glass Beads	42
26.	Effect of Probe-to-bubble-path Separation on Apparent Bubble Volume	46
27.	Bubble Velocity as a Function of Bubble Volume for 60 Mesh Glass Beads	47
28.	Bubble Velocity as a Function of Bubble Volume for 80 Mesh Glass Beads	48
29.	Bubble Velocity as a Function of Bubble Volume for 120 Mesh Glass Beads	48
30.	Bubble Velocity as a Function of Bubble Volume for 170 Mesh Glass Beads	49
31.	Effect of Particle Size on Bubble Velocity/Bubble Volume Factor	49

LIST OF TABLES

No.	Title	Page
1.	Glass Bead Size Fractions	21
2.	Size Analyses of Mixtures	40
3.	Average Bubble Volumes for Glass Beads in a $5\frac{1}{2}$-in.-dia Column	45
4.	Observed Bubble Diameters for Glass Beads in a $5\frac{1}{2}$-in.-dia Column	45

THE EFFECT OF PARTICLE SIZE ON THE PROPERTIES OF GAS-FLUIDIZED BEDS

by

K. S. Sutherland

ABSTRACT

The development of a continuous method for determining changes in particle size and particle size distribution in fluid-bed systems has been studied experimentally. Differential pressure measurements were employed to study the effects of solid particle size on the behavior of gas-fluidized beds. The relevant bed properties are briefly described and a review given of previous work on the study of fluidized-bed quality. It is shown that, within certain limitations, measurements of bed quality can be used to indicate changes in particle size. Gas-bubble velocities, while increasing in proportion to the square root of bubble diameter, are also shown to be dependent on particle size, increasing as the particle size decreases.

1. INTRODUCTION

In the course of chemical reactions taking place in gas-fluidized beds, the size of the particles may change as a result of several mechanisms. Some changes may be expected and will be allowed for in the design of the reaction system. Other changes may be unexpected, and these will almost certainly be unwanted. Examples of such unwanted changes are the formation of lumps, which may cause the bed to lose its fluidization characteristics, and the production of an excessive quantity of fine particles, which may result in loss by elutriation of valuable solid material, or cause operating difficulties in the equipment for off-gas treatment.

At present, little can be done to observe changes in particle size and size distribution short of sieve analysis, which is time-consuming and may be difficult under some conditions, such as in the presence of high levels of radioactivity. Attempts to develop more rapid means of determining particle size changes by observation of fluidized-bed properties have so far been relatively fruitless. However, if such a method were available it would be a valuable process operation tool. This study was therefore undertaken to examine the effects of particle size on some of the mechanical properties of gas-fluidized beds to discover if one of

these properties could be used as an indicator of changing particle size. A promising method used previously has been the observation of the variations in pressure drop between two probes, mounted one above the other in the fluidized bed, and this method has been adopted for the present study.

2. THE EFFECT OF PARTICLE SIZE ON THE PROPERTIES OF FLUIDIZED BEDS

2.1 The Characteristics of Fluidization by Gases

To examine the effects of changing particle size on the behavior of gas-fluidized beds, it is first necessary to consider all the properties of fluid-bed systems that are likely to be affected. The distinctive characteristics of fluidized beds that make fluidization such a convenient processing tool are by now well-known and need only be summarized as follows:

a) Fluidized solids behave as a liquid, with a definite "hydrostatic" head, and can easily be fed to, and removed from, a reactor.

b) Equipment is relatively simple, with few moving parts, and fluidized-bed processes are quite easily controlled.

c) Fluidization begins at a particular gas velocity, which is characteristic of the properties of the gas and solid involved; this velocity is considerably less than the terminal velocity of the average-sized particle.

d) The range of gas flow rates over which fluidization is possible is limited, at the lower end by the minimum fluidization velocity, and at the upper end by slugging and/or entrainment of the bed particles.

e) The pressure drop across a fluidized bed remains approximately constant, at a value equal to the bed weight per unit area, as the gas flow is increased above the minimum fluidization flow rate; this constant pressure drop would then be less, for the same gas flow rate, than that for the same material constrained as a fixed bed.

f) Gas-fluidized beds are normally agitated by bubbles or pockets through which gas is continuously flowing and which cause rapid, solid movement through the bed.

g) At any given instant, the volume of gas in excess of that required to fluidize the bed is believed to be present as bubbles, although there may be constant interchange of gas between these bubbles and the rest of the bed.

h) Rapid solid circulation results in uniform solid composition and temperature throughout the bed and promotes heat transfer between the bed material and a heat exchange surface.

i) The fine subdivision and consequent higher surface area of the bed material, as compared with a fixed bed, give a higher rate of heat and mass transfer between gas and particles, although the transfer coefficients are little different in the two cases.

j) As the fluidizing gas velocity increases, the heat transfer rates between the bed and a heat exchange surface at first increase, then pass through a maximum value, and finally decrease.

k) Although solid composition and temperature are usually uniform throughout a fluidized bed, a system having thermal and concentration gradients can be produced; this can be done by tapering the bed, by using baffles, or by using several beds in series.

l) Fluidized beds offer resistance to the passage of a solid object through them; this resistance, which is characteristic of bed conditions, is analogous to the viscosity of the liquid.

m) Fine particles above a certain concentration are elutriated from a bed according to a first-order law, the concentration of fines in the off-gas being proportional to that in the bed.

2.2 The Effect of Particle Size on Bed Properties

Since so many of the properties of a fluidized bed are interdependent, it is often difficult to separate the individual effects of average particle size and particle-size distribution on the mechanical and transfer properties of the bed, but the following general observations may be made:

a) The minimum fluidization velocity is directly proportional to the square of the average particle diameter, and is somewhat affected by the width of the particle-size distribution.

b) A large average particle size is more conducive to slugging than a small value, since the ratio of slugging velocity to minimum fluidization velocity increases as the average particle size decreases; however, a bed of very fine particles is prone to channeling, and the best fluidization conditions are usually obtained with a wide size distribution.

c) A limitation of the fines content of a wide size distribution is the gradual elutriation of the smallest particles at the velocity required to fluidize the largest particles.

d) The pressure drop across a fluidized bed is unaffected by particle size, although in the prefluidized (i.e., fixed-bed) state it is inversely proportional to the square of the average particle size.

e) The void fraction of the incipiently fluidized bed is inversely proportional to particle diameter for close cuts of particle size, and is higher for a close cut than for a wide distribution with the same average particle size.

f) The bed "viscosity," as measured by methods developed for liquids, is strongly dependent on void fraction, and is especially affected by fines concentration (a small proportion of fines added to a bed of coarse particles greatly reduces the bed viscosity).

g) Heat and mass transfer rates between particles and fluid are markedly affected by particle size, since the available surface increases as particle diameter decreases (the actual transfer coefficients are not affected, however, and since instantaneous transfer rates are difficult to measure, this property of the bed is unlikely to provide a simple indication of particle-size changes).

3. QUALITY OF FLUIDIZATION

No mention has been made so far of that property of a fluidized bed called the "quality" or "uniformity" of fluidization. As defined by Morse,[1] "quality of fluidization is ... the uniformity of particle disperison and the uniformity of gas velocity in a boiling bed. The water-fluidized bed of sand approaches perfect quality. The bed that slugs or channels badly is at the other extreme of quality. The bed in which the gas pockets remain small and well distributed, with a steady, even, overall boiling of the bed, is intermediate in uniformity, but perhaps optimum in the balance between uniformity and the requirement of mixing and boiling in order to control temperature."

Although considerable experimental effort has been devoted to a study of bed uniformity, a quantitative value for quality of fluidization has proved difficult to define. A fluidized bed is a heterogeneous system, but, the above definition indicates that the more a bed resembles a homogeneous fluid, the greater will be its uniformity. Whether large or small, the gas bubbles in a fluidized bed give it its appearance of gross heterogeneity; a study of the quality of a bed therefore reduces to a study of its bubbling properties. As indicated above, a bubble-free bed may not be ideal from all points of view, since particle movement in a gas-fluidized bed does not occur in the absence of gas bubbles.[2-4]

The value of some early theoretical studies of bed quality[1,5,6] was reduced by the nonavailability to their authors of some of the more recent studies of the actual nature of gas-fluidized beds, and by acceptance

of Wilhelm and Kwauk's term "aggregative fluidization" to describe such beds. The most valuable contribution was that of Rice and Wilhelm[6] who developed a set of equations governing the stability of bed-fluid "interfaces" (although they decided that it was the upper surface of a bubble that was unstable). These equations have been further developed by Romero,[7,8] who rearranged them into dimensionless group form, but they can still be used only to distinguish between "particulate" and the so-called "aggregative" fluidization.

Several experimental methods have been used to study bed uniformity, of which the more common are as follows:

a) Absorption of light or other radiation by the bed.[9-18]

b) Determination of bed viscosity.[19-28]

c) Variation in capacity of an electrical condenser immersed in the bed.[29-33]

d) Fluctuation in bed pressure drop.[14,17,34-42]

Other methods have involved following the impact of particles on a diaphragm connected to a piezoelectric crystal,[43] a study of bed surface fluctuations,[44] use of a thermistor probe[45] or hot-wire anemometer,[8] and cinephotography.[46,47] Additional information on bed quality can also be obtained from the kinetics of chemical reactions carried out in fluidized beds, as compared with those carried out in fixed beds under similar conditions.[48-53] This method, however, produces little more useful information than that some of the reacting gas has "by-passed" the fluidized bed.

None of the above-mentioned methods is perfectly satisfactory as a measure of fluidization quality. Viscosity measurements involve the insertion into the bed of a paddle or similar device which, by its presence, as well as its rotation, interferes with the bed behavior in the area that it is exploring. Similarly, a small capacitor will also interfere with local behavior. In addition, the capacity method is limited to nonconducting solids. The radiation-adsorption methods overcome this difficulty of interference with bed behavior, but they cannot, in general, distinguish between the effect caused by, say, one large bubble crossing the beam and that of two bubbles, each half the size of the large bubble, crossing together. The equipment used is quite elaborate and more costly than that for the other methods.

Viscosity, capacity, and absorption measurements are limited to a particular region of the bed, which may be quite small with respect to the bed size. If the bed is deep or of large diameter, such determinations

cannot give a reliable picture of the overall behavior. The pressure-drop fluctuation method may not have this limitation, but it may also have the inability to distinguish between one large bubble and several small ones in the zone of study.

From the point of view of ease of experimentation, the pressure-drop fluctuation method is probably the best of those used so far. In addition, it has the advantage of being dependent upon the bubbling characteristics of the bed to a greater degree than most of the other methods, since at any given instant, the pressure drop across any region of a fluidized bed is directly proportional to the weight of solid in that region. The presence of bubbles will alter this pressure drop by an amount related to the bubble volume, since the bulk density of the dense phase surrounding the bubbles remains approximately constant.

Comparatively few of the forty-odd references to bed quality contained much useful information. The papers commonly describe in detail the experimental methods used, but fail to give much data on the effect of bed properties on uniformity of fluidization. There is frequently conflict between the results of various authors; for example, most authors agree that the wider the particle size distribution, the more uniform the bed whereas Tyuryaev et al.[41] find their index of heterogeneity to be independent of the width of distribution.

The end product of most methods of study is a single trace on a recorder chart. For a given set of conditions, this trace will have a roughly constant frequency of oscillation about a mean value, and a roughly constant maximum amplitude of oscillation, but will, in general, be highly irregular in shape. From such traces, varied "uniformity indices" have been obtained, on the assumption that amplitude and frequency are characteristic of the corresponding bed conditions. The usual index involves an average deviation from the mean value divided by the frequency, so that a low value for the index indicates good uniformity, and a high value indicates poor quality. Because of the uncertainty in the measurement of frequency, there has been increasing use of an index evolved from the rate of change of the variable or "intensity of fluctuation," exemplified by the work of Brazelton[34] and Fitzgerald.[36] The available evidence does not indicate that either of these two types of index is superior to the other.

The following general comments summarize the various sets of published results.

a) Bed quality is reduced as the fluidization velocity is increased.

b) For a given average particle size, a wide-size cut seems to give more uniform fluidization than a narrow one.

c) For narrow size cuts, a small particle size tends to give a more uniform bed than a large size.

d) The uniformity of a bed of coarse particles is improved considerably by adding a small quantity of fines, but a corresponding addition of coarse particles to a bed of fine particles has little effect.

e) Increase in bed height, within limits, is said not to affect the uniformity at a fixed distance above the distributor.

f) Uniformity decreases with increasing distance from the distributor.

g) A porous plate distributor, especially one for which the pressure drop across it is a significant fraction of that across the bed, gives more uniform fluidization than wire screens, cone inlets, or perforated plates.

h) Uniformity decreases as the ratio of particle-to-fluid density increases.

4. PRESSURE-DROP FLUCTUATIONS IN A FLUIDIZED BED

4.1 Previous Experimental Methods

Rapid changes in pressure drop across all or part of a bed have been followed by recording the movements of a thin diaphragm connected to probes immersed in the bed. This has been done in two ways. Henwood and Thomas[37] and Reboux[38] used a single probe connected to one side of the diaphragm, which constituted one (movable) plate of an electrical condenser having a fixed plate mounted close to it. The movement of the diaphragm altered the capacity of the condenser, and the variations were studied either by photography of an oscilloscope trace,[38] or by a high-speed recorder and an integrating meter.[37] In both cases, the other side of the diaphragm was maintained at approximately the same average pressure as that on the recording side.

The second method involves two probes, one connected to the space on each side of the diaphragm, the movement of the diaphragm being indicated by strain gages.[34-36,39] Shuster and Kisliak[39] had the probes connected across the entire bed, whereas Brennecke[35] had one probe always above the bed, and then placed the second probe at various bed levels. Both obtained a chart record of the voltage fluctuations produced in the strain-gage bridge network, and determined uniformity indices based on planimeter-measured chart areas.

The continuing work reported by Brazelton,[34] Fitzgerald,[36] and Levitz[54] has used the same two-probe-and-strain-gage system, which

provides a record of the intensity of fluctuation by means of an emf squaring device, such as a heater-thermocouple junction.

The last-mentioned method has produced some encouraging results, since some effect of particle size can be observed, and a direct reading is given without need for subsequent analysis of a chart record.

4.2 The Effect of Gas Bubbles on Pressure-drop Readings

In a bed of particles that is maintained at the point of incipient fluidization, the pressure drop across a region is effectively equal to the weight of bed material in that region, divided by the cross-sectional area of the bed. If the gas velocity is increased just enough to cause a bubble to rise through the bed, then (since it can be assumed that the bulk density of the fluidized material surrounding the bubble does not change significantly) the pressure drop across the region should decrease in the ratio of bubble volume to probe-region volume. When the bubble leaves the region, the pressure drop will return to its original value.

Thus, if the indicating device is inertialess, the record produced by a succession of bubbles passing through the region should be a steady maximum value with a series of troughs representing the bubbles. If only one bubble at a time passes through the zone under examination, the depth of each trough will be proportional to the volume of the corresponding bubble, and the width of the trough will be inversely proportional to the bubble velocity.

The presence of more than one bubble in the region at any instant will complicate this simple picture. Two bubbles passing through together will produce the same trough in the trace as a single bubble of the same total volume moving at the same velocity. However, since there is some indication that the speed of a bubble is related to its size,[55,56] it is likely that the larger bubble will be travelling faster and so could possibly be distinguished by a narrower trough.

The pressure-sensing device will have some interia, however, so that the initial and final surges of each bubble may exceed the mean effect lines on the trace, but it should be possible to follow the trace for a gently-bubbling bed. When the bubbling intensity increases, the inertia of the bed may begin to exert an effect on the pressure traces, since the solid material may, to a certain degree, be compacted ahead of a bubble, and expanded behind it. This will produce a more complicated trace, and the complexity will increase as the bubbling rate increases. For a system in which bubbles can be generated at any required frequency and of known size, it may be possible to reproduce traces obtained with randomly-fluidized beds, and so understand the mechanism responsible for these traces.

It seems reasonable to assume that the pressure-drop trace produced by probes situated on the bed axis would be the same as that produced by probes situated at the wall, provided that the bed does not have too great a diameter. For large beds, however, instantaneous pressure drops between any two levels may vary widely between axial and wall regions.

Bubbling in a fluidized bed is frequently assumed to be a random process, but this may not be true. When bubbling is not random in position, the methods of uniformity analysis that rely on point determinations will not give as correct a picture as will the overall effect of pressure-drop fluctuation.

5. EXPERIMENTAL SYSTEM

5.1 Apparatus

The experiments described in this report were conducted in Lucite columns with air as the fluidizing gas. The arrangement is illustrated in Figure 1. The air was supplied from a 100-psig main through a humidifier to a pressure-reducing valve. The flow rate was measured by a bank of rotameters, each of which could be used individually, and the rate was controlled by valves downstream of the rotameters. In this way, the pressure in the rotameters could be maintained at a constant value regardless of the pressure drop across the fluidized bed in use.

Figure 1

DIAGRAM OF APPARATUS

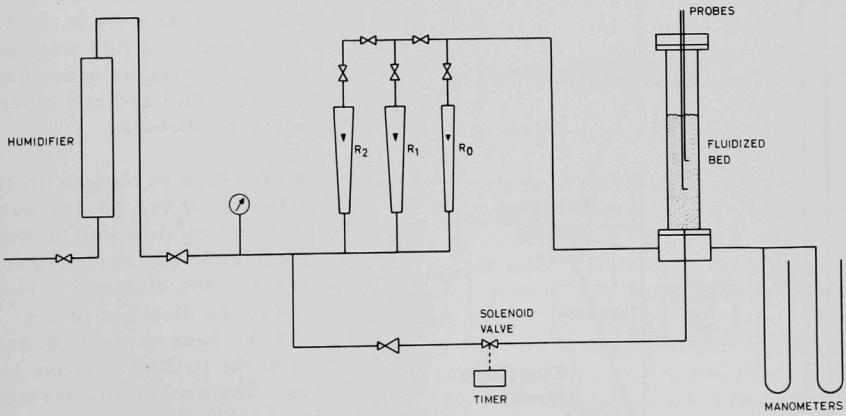

108-7494

Air entered the fluidized bed units at the side of the inlet box, to which the columns were connected by a flanged joint with an O-ring seal.

A porous metal distributor plate was mounted between the inlet box and the column, the seals being made of flat rubber gaskets. The columns were of 3-, $5\frac{1}{2}$-, and 11-in. internal diameter, in various lengths, with flange and O-ring joints between the sections when more than one were used.

Each inlet box had a pressure tapping leading to two manometers in parallel, one filled with mercury, and one with a fluid whose specific gravity was 2.95. By means of these manometers, the pressure drop across both the bed and the distributor plate could be determined. The pressure drop across the distributor alone was measured before any bed material was in place, and the appropriate values were subtracted from the overall figures to give the pressure drop across the bed alone. This eliminated the need for additional purging air flows that would be required for a pressure tapping above the distributor plate.

Figure 2
SKETCH OF PROBES

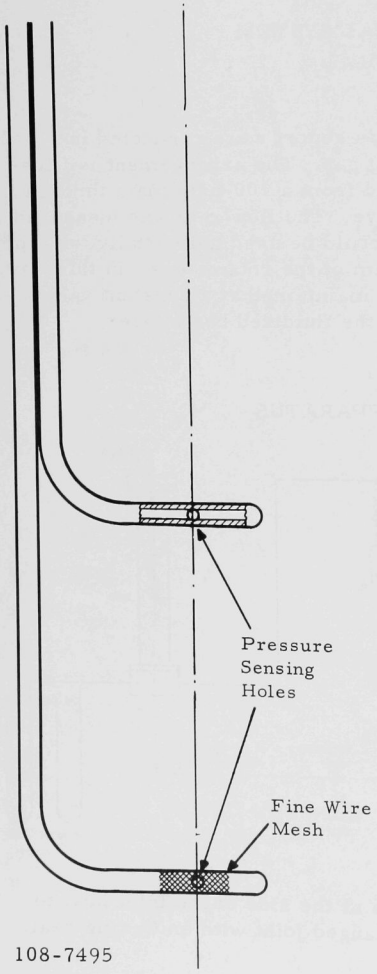

Provision was also made in each inlet box for an additional air supply to the bed through a $\frac{1}{8}$-in.-bore plastic tube, whose end was flush with the top of the distributor plate and at its center. The air was taken from the low-pressure side of the main reducing valve through a second reducing valve to a solenoid-operated check valve. The solenoid was energized by an electronic timer delivering pulses continuously variable from 0.01 to 1.1 sec. In this way, individual bubbles of various sizes could be injected into a fluidized bed otherwise effectively free of bubbles.

The pressure variations in the bed were detected by two probes suspended from a clamp mounted on the column. The clamp was designed to permit adjustment of the distance between the two probes, the distance of the probes above the base of the bed, and the position of the probes relative to the bed axis. The probes themselves were made of steel tubes of approximately $\frac{1}{16}$-in. bore, the lower inch or so of each being bent at right angles to the rest of the probe (see Figure 2). The lower end was sealed, and a hole of the

same bore was drilled through the tube horizontally about $\frac{1}{4}$-in. from the end. These pressure tappings were then covered with fine wire mesh to prevent the entry of solids.

The two probes were connected, by lines that were as short as possible and of equal length, to the high- and low-pressure sides, respectively, of a differential pressure transducer (Consolidated Electrodynamics Corporation, Type 4-315). Separating the high- and low-pressure sides was a thin diaphragm which moved as the differential pressure changed. The movements were detected by a strain gage fixed to the diaphragm; the variations in resistance of the strain gage were converted to variations in potential in a bridge network, shown in Figure 3. A 6-volt battery and voltage divider were used to provide a steady 5-volt source to the bridge, which also had a zero-adjustment circuit. For most experiments, the output from the transducer, which was of the order of a few millivolts, was detected directly by a Bristol single-pen chart recorder, with chart speeds up to $\frac{2}{3}$ in./sec. Use was also made of a Honeywell Visicorder, with a record made by a spot of light, reflected from the mirror of a miniature galvanometer, on photosensitive paper. This system needed a DC amplifier because of its lower sensitivity, but could be operated with paper speeds up to 50 in./sec, and also had provision for several inputs, enabling the use of auxiliary timing units. One input was an electronic timer giving regular pulses at 0.01-, 0.1- and 1-sec intervals; another input detected (via a relay) the open time of the solenoid valve that was used to generate single bubbles.

Figure 3

ELECTRICAL CIRCUITS AND BLOCK DIAGRAM

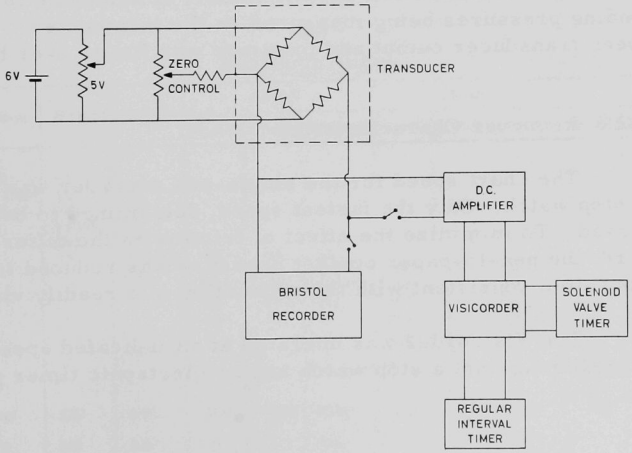

108-7496

5.2 Apparatus Calibration

5.2.1 Rotameters

The three rotameters used in these experiments had the following flow ranges:

R0: 0.025-0.45 scfm when calibrated at 10 psig;

R1: 0.3-2.4 scfm when calibrated at 50 psig;

R2: 2-18 scfm when calibrated at 50 psig.

The rotameters were calibrated against at least two of a set of three gas meters, at the pressures indicated above. During the calibration, a set of readings was also taken of the pressure drop across one of the porous distributor plates for the 3-in.-dia bed. These values were plotted on a single graph for all three rotameters to ensure that a smooth continuous curve was obtained. This demonstrated the lack of error between one gas meter and another.

5.2.2 Transducer Calibration

The relationship between transducer output voltage and applied differential pressure was determined at the beginning of the study and repeated during its course to ensure constant behavior. The transducer and the oil manometer were connected to the high-pressure air line through a reducing valve, and the pressure adjusted by means of a controlled-leak valve. The output of the transducer was then determined on the Bristol recorder and by a standard cell potentiometer, at values up to 10 mV, the corresponding pressures being measured on the manometer. The relationship between transducer output and pressure was linear over the entire range.

5.2.3 Recorder Characteristics

The chart speed for the single-pen recorder was measured against a stop watch. Only the fastest speed, determined to be 0.674 in./sec, was used. To minimize the effect of friction on the differential pressure record, the pen-to-paper contact pressure was reduced to as low a value as possible consistent with the production of a readily visible trace.

The Visicorder was operated at an indicated speed of 10 in./sec. Calibration against a stop watch and an electronic timer gave a value of 10.54 in./sec.

5.2.4 Bubble Generator Calibration

The bubble generator was mounted initially to produce bubbles under water. The unit was then calibrated at several timer settings by determining the volume of air passed by a known number of pulses. The limit was also established for the production of a single bubble per pulse rather than a series of bubbles. This limit was checked in a fluidized bed and found to apply quite closely. The bubble generator characteristics were determined at intervals during the study to check on uniformity.

5.3 Fluidized-bed Materials

Apart from a few tests made with copper shot, all the experiments were performed using glass beads as the fluidized-bed materials. The size range of the beads was from 25 to 270 mesh. Some initial work was done with a mixture of glass beads -40 +60 mesh. After this, the available material was carefully screened into six fractions, with intended size distributions as follows:

35 mesh fraction -30 +40 mesh (420 to 595 microns);
45 mesh fraction -40 +50 mesh (297 to 420 microns);
60 mesh fraction -50 +70 mesh (210 to 297 microns);
80 mesh fraction -70 +100 mesh (149 to 210 microns);
120 mesh fraction -100 +140 mesh (105 to 149 microns);
170 mesh fraction -140 +200 mesh (74 to 105 microns).

Actual screen analyses for the six fractions are shown in Table 1, with corresponding mean particle diameters. Bead densities determined by using a specific-gravity bottle are listed in Table 1.

Table 1

GLASS BEAD SIZE FRACTIONS

	35 Mesh	45 Mesh	60 Mesh	80 Mesh			120 Mesh			170 Mesh		
				Drum A	Drum B	Combined	Drum A	Drum B	Combined	Drum A	Drum B	Combined
+30 w/o	0.2											
-30 +35 w/o	11.8	0.1										
-35 +40 w/o	66.7 (94.7)	1.0										
-40 +45 w/o	16.2	13.4	0.2									
-45 +50 w/o	5.1	59.8 (97.7)	1.1									
-50 +60 w/o		24.5	44.5									
-60 +70 w/o		1.2	35.9 (92.8)	0.3	0.3	0.2						
-70 +80 w/o			12.4	9.4	6.3	7.3	0.1	0.6	0.2			
-80 +100 w/o			5.9	70.7	78.9	78.9 (98.1)	1.0	1.6	1.3			
-100 +120 w/o				21.3	12.4	11.9	19.3	76.4	67.2	0.4	0.1	0
-120 +140 w/o				3.3	2.1	1.7	61.4	15.5	21.7 (96.6)	9.1	34.2	30.1
-140 +170 w/o							13.0	4.2	7.7	39.3	41.4	47.6 (98.3)
-170 +200 w/o							5.2	1.7	1.9	45.4	22.6	20.6
-200 +230 w/o										2.5	0.8	0.7
-230 +270 w/o										3.3	0.9	1.0
Mean particle diameter, mm	0.445	0.317	0.231	0.159	0.160	0.160	0.114	0.130	0.126	0.082	0.097	0.096
Bead density, gm/cc	2.50	2.49	2.43	-	-	2.45	-	-	2.45	-	-	2.45

Some difficulty was experienced in the early stages of the work in obtaining consistent size-analysis data. The difficulty was caused by difference in behavior between available standard screens of nominally the same mesh. Because accurate size analysis standards were vital to the study, considerable effort was expended in establishing a set of screens that was both consistent and reasonably accurate. The optimum size of sample and the optimum sieving time for accurate analysis were also established, at 50 gm and 20 min, respectively. All size analyses are given in terms of this set of screens and so are at least self-consistent, if not absolutely accurate.

5.4 Experimental Method

For most of the tests performed during this study, three types of data were obtained. Firstly, the variation in bed pressure drop with gas flow rate was observed over as wide a range as possible for each system. From these data, the value of the air flow rate necessary just to fluidize the bed was closely approximated. Recorder traces were then obtained of the differential pressure drop at several air rates up to at least 50% above the minimum fluidization rate, in order to represent the general state of the bed when fluidized. Finally, a set of traces was obtained with single bubbles injected at the bottom of the bed, the general air flow being just sufficient to fluidize the bed gently without producing unwanted bubbles.

For the pressure-drop data, and for the traces at the lower air flow rates, it was important that the condition of the bed be reasonably reproducible from one reading to the next. The most satisfactory way of achieving this was to fluidize the bed vigorously before each reading and then reduce the air flow to the required value at an approximately constant rate. This method also eliminated variable meniscus errors in reading the two manometers.

The records of the general fluidization traces were obtained in sufficient length (at least 12 in.) to permit subsequent analysis of the curves. The bubble traces were repeated six times for each set of experimental conditions, sufficient time being allowed between the bubble injections for the bed to return to its original condition.

Additional data recorded where necessary included the weight of solid particles used in each test, and the change in position of the upper surface of the bed during bubble injection as a measure of the bubble size. A further indication of a bubble's size was obtained by observing its approximate diameter as it burst through the upper surface of the bed.

5.5 Experimental Program

The variables covered during this study were as follows:

a) Bed diameter: 3, $5\frac{1}{2}$, and 11 in.;

b) Bed depth: up to 30 in.;

c) Bed particle size: 35 to 170 mesh;

d) Particle size distribution;

e) Particle density: 2.5 and 8.9 gm/cc;

f) Gas flow rate;

g) Probe position and separation from bed axis.

Some initial experiments were performed with a -40 +60 mesh cut of glass beads to develop satisfactory techniques for determining the minimum fluidization velocity, and to determine the most satisfactory probe positions and spacing for the initial tests.

The first of the main group of experiments employed bed depths of 15 in. in each of the three bed diameters using all six size fractions where possible, to show the effect of bed diameter, particle size, and air flow rate. The next set tested the effect on injected bubble traces of moving the probes horizontally away from the center line of the beds, for the $5\frac{1}{2}$- and 11-in.-dia tubes. Since the bubbles were always injected along the bed axis, these experiments showed the degree of influence on the differential pressure trace of bubbles at various distances from the probes.

The effect of denser particles was observed by using copper shot (with approximately three times the density of the glass beads) in the 3-in.-dia bed. Only one size of copper shot was used.

The fourth group of experiments tested the effect of bed height and vertical probe position and separation on the fluidization and bubble traces. These tests were made in the $5\frac{1}{2}$-in.-dia tube, with bed heights up to 30 in., and with four of the size fractions (60, 80, 120, and 170 mesh).

The last series of experiments examined the effect of changing particle size distributions. The individual fractions were mixed in a variety of ways in known proportions to simulate the appearance of fines in a bed of coarser particles or of larger particles in a bed of small ones, and to simulate a gradual change in average particle size.

6. PRESENTATION AND DISCUSSION OF RESULTS

6.1 Treatment of Data

To convert the general fluidization traces on the recorder charts into usable data, some easily measurable characteristic of the traces had to be found. The properties that might be suitable are the amplitude of the trace, the average value of pressure drop indicated by the trace, the frequency of oscillation, and the degree of oscillation or sinuosity of the trace.

The time average of the quantity of solid in the region of the bed between the probes, and hence the pressure drop across them, depend only on the bed expansion, and therefore to a great extent on the fluid velocity. The average value of the trace would thus appear to be relatively insensitive to particle size changes, and so this characteristic was of no value.

The maximum amplitude of the trace was easily measured, but it was observed that, especially at air rates not much greater than the minimum fluidization value, occasional peaks were much higher than the rest, making a measurement of maximum amplitude too uncertain.

In most traces, no obvious frequency was readily detectable, although Fourier analysis of the traces might have produced a characteristic frequency. The sinuosity of the curve is related to the various frequencies combined in the trace and is relatively easily measured. It was therefore adopted as the trace characteristic best able to enumerate the quality of the fluidized bed producing the trace.

Figure 4
TYPICAL FLUIDIZATION TRACES

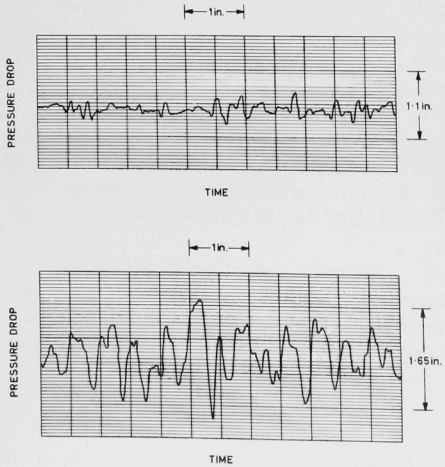

108-7497

The oscillations of the trace result from changes in pressure drop between the probes, the changes being caused by the passage of gas bubbles through the probe zone. Large bubbles cause large oscillations, so that the best fluidization quality, according to Morse's definition, would correspond to a gently oscillating trace, of small amplitude. A bed having many large bubbles would be of poor quality and may produce a more sinuous trace. The sinuosity of the trace may thus be considered to be a direct measure of bed quality. Figure 4 shows two typical traces, the upper one corresponding to a bed

of reasonably good quality, the lower one to a bed of much poorer quality, as evidenced by visual inspection.

The sinuosity of a given trace can be measured by the actual length of the line traced on the chart, because of an important characteristic observed in the traces. The line length obtained from a curve with low frequency and large amplitude could be the same as that obtained from a curve with a high frequency and small amplitude; each curve would then have the same apparent sinuosity as measured by line length, but one would be much more sinuous than the other. However, a reduction in quality of a fluidized bed has the effect of adding on to the high-frequency, low-amplitude oscillations the characteristic of a bed of good quality, a lower-frequency oscillation of greater amplitude corresponding to the larger bubbles causing the reduction in quality. This behavior is shown to some extent in Figure 4. Although some reduction in quality is evident in the upper curve, the effect of the larger bubbles is much more apparent in the lower one.

The sinuosity of the recorder traces has thus been used in this study as a direct indicator of bed quality. It was measured in terms of the length of the trace, and in some cases this was done directly by means of a map measurer. This instrument was run over the trace for a fixed chart length of 6 in., which corresponds to a time interval of 8.9 sec. Since it was almost impossible to follow the line accurately, three measurements were made and the average value determined. The process was then repeated on another 6-in. length of the same chart to give two values of sinuosity for each set of conditions.

Most of the sinuosity measurements were obtained in terms of "line-cut counts." As shown in Figure 4, the chart on which the traces were made was divided into 0.5-in. (0.74-sec) intervals along the time axis, and by lines parallel to the time axis spaced 0.055 in. apart. These latter lines were perpendicular to the direction of movement of the recorder pen; therefore, the more rapid the pen movement (i.e., the more sinuous the curve), the more of these lines would be crossed by the pen in any given period of time. Accordingly, the sinuosity was determined by counting the number of times the trace crossed any of the lines parallel with the time axis within a 6-in. length of chart, and the line-cut count was repeated on a second length, again to give two measurements of sinuosity.

In the sections that follow, the terms "sinuosity," "line-cut count," and "line length" will therefore be used interchangeably as measures of "bed quality."

A generalized trace for a single injected bubble, typical of those obtained at low fluidizing flow rates, is shown in Figure 5. The regions AB and FG represent the gently-fluidizing, bubble-free bed. As soon as

the solenoid valve was opened, a pressure wave passed through the bed, and this damped wave is indicated by BC. When the bubble reached the lower probe, at D, the differential pressure fell as the amount of solid in the probe zone decreased, and then rose (to E) as the bubble left the zone. In nearly all cases, a marked rise in pressure (shown at EF) was observed after the bubble had left the probe zone. This was probably caused by the collapse of the bed as the bubble burst. In some cases, a slight rise in pressure was observed just before the bubble reached the probe zone; this may have been due to compaction of particles ahead of the bubble.

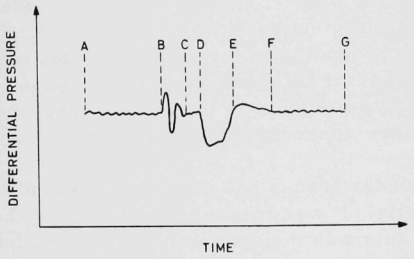

108-7498

Figure 5

A GENERALIZED BUBBLE TRACE

The parts of the trace used to give information on bubble behavior were the interval BD, between injection and the time of reaching the probe zone, and the depth of the trough in the interval DE. The first of these is used to obtain bubble velocities, and the second as a measure of bubble size. As bubble injection occupied a finite time (from 0.036 to 0.236 sec), it is assumed that the rate of rise of the top of the bubble during formation was not markedly different from the bubble-rise velocity.

6.2 Measurements of Fluidization Quality

6.2.1 Effects of Particle Size and Bed Diameter

The tests made in this part of the program are as follows:

3-in.-dia beds; 35, 45, 60, 80A, 80B, 120A, 120B, 170A, and 170B mesh glass beads;

$5\frac{1}{2}$-in.-dia beds; 45, 60, 80A, 80B, 120A, 120B, 170A, and 170B mesh glass beads;

11-in.-dia beds; 60, 80, 120, and 170 mesh glass beads.

The suffixes A and B for the 80, 120, and 170 mesh material represent, for each fraction, the contents of two separate drums of slightly differing particle size. These two lots had to be combined to give enough material for the 11-in.-dia beds. There was not enough 35 mesh material

for the $5\frac{1}{2}$-in. bed, nor enough 45 mesh material for the 11-in. bed. The minimum fluidization velocities for all these tests, as determined from plots of pressure drop against air flow rates, are shown in Figure 6. Here they are plotted against the average particle diameter, and the line drawn on the graph has a slope of 2, in agreement with the fundamental dependence of the minimum velocity on the square of particle diameter. The average particle diameter was that given by the relation

$$\bar{d}_p = \left(\sum \frac{x_i}{d_i} \right)^{-1},$$

where x_i is the weight fraction of material between two adjacent sieve sizes, and d_i is the mean size of these two sieves.

Figure 6

THE DEPENDENCE OF MINIMUM FLUIDIZATION VELOCITY ON AVERAGE BED-PARTICLE SIZE

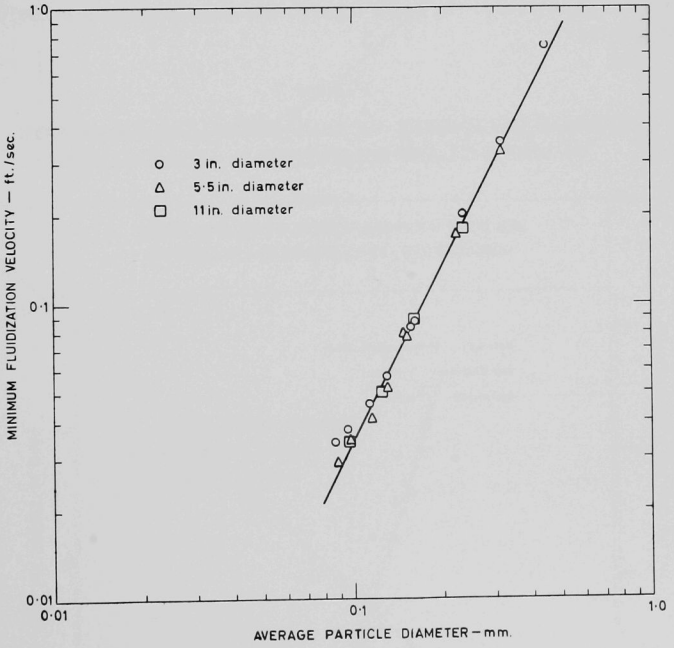

108-7499

The correlation between velocity and the square of the mean particle diameter is good, although there is a slight indication of a departure from linearity for the smallest particle sizes. This divergence may be accounted for by a more pronounced effect of static electrical

charges with the smaller material. Because of the need to use relative velocities in comparing later results, the minimum fluidization velocities had to be known with some confidence. Despite the inherent difficulties involved in measuring such velocities,[57] the method adopted here has given values quite satisfactory for their purpose.

The actual size fractions employed in this study, as shown in Table 1, were less closely sized than was intended, although each has well over 90 w/o within three adjacent sieve fractions. As a result of this wider range, there was some overlap between successive fractions, especially between the 120 and 170 mesh material.

The results of the line-cut count analyses are shown in Figures 7 to 16. A typical analysis for one size fraction (60 mesh) and one bed size (3-in. dia) is shown in Figure 7, in which the number of line-cut counts in 6 in. of chart length is plotted against air flow rate. Similar examples are given in Figure 8 and 9 for 80 mesh, $5\frac{1}{2}$-in. dia, and 60 mesh, 11-in. dia, respectively. In each figure, the data points are included to show the scatter.

Figure 7

TRACE INTENSITY VERSUS AIR FLOW RATE FOR 60 MESH GLASS BEADS, 11-in.-DIA COLUMN

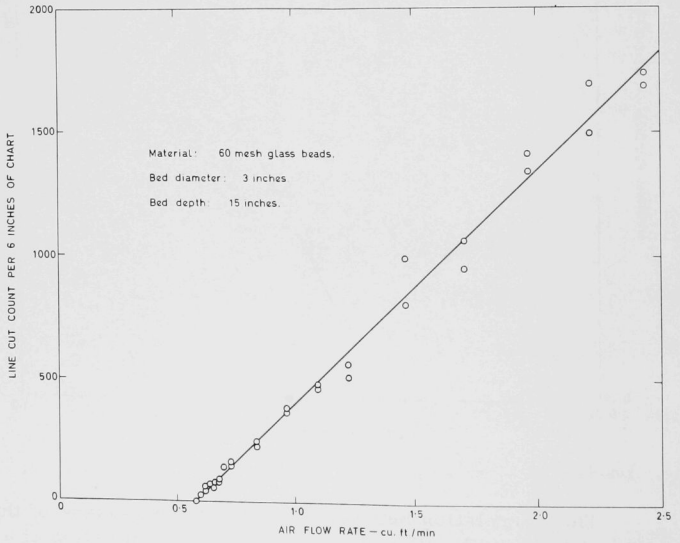

108-7500

Figure 8

TRACE INTENSITY VERSUS AIR FLOW RATE FOR
80 MESH GLASS BEADS, 5.5-in.-DIA COLUMN

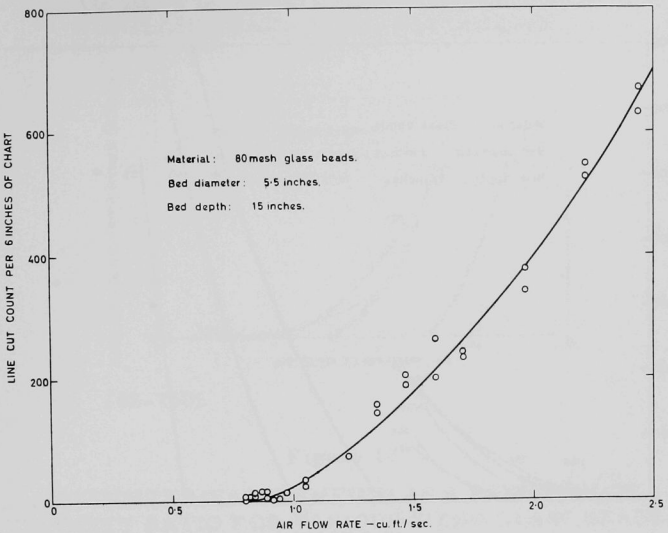

108-7501

Figure 9

TRACE INTENSITY VERSUS AIR FLOW RATE FOR
60 MESH GLASS BEADS, 11-in.-DIA COLUMN

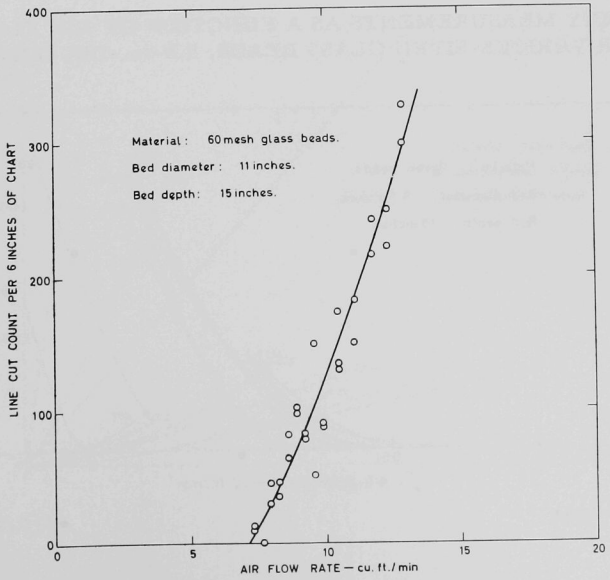

108-7509

Figure 10

INTENSITY MEASUREMENTS AS A FUNCTION OF AIR FLOW RATE FOR VARIOUS-SIZED GLASS BEADS, 3-in.-DIA COLUMN

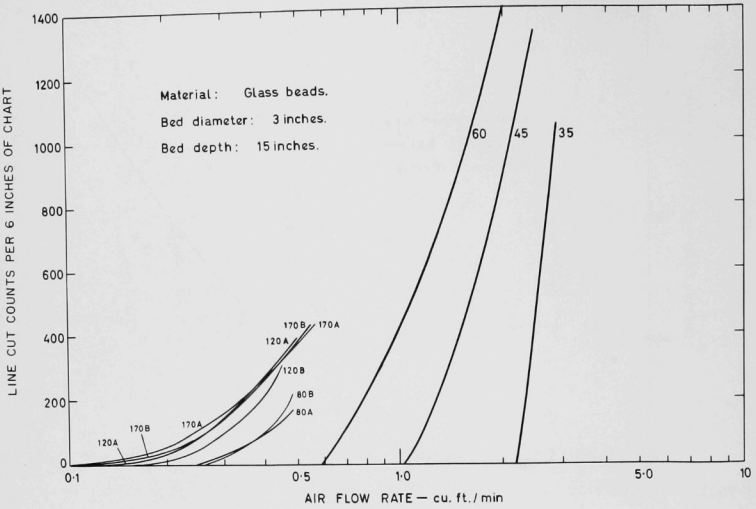

108-7503

Figure 11

INTENSITY MEASUREMENTS AS A FUNCTION OF AIR FLOW RATE FOR VARIOUS-SIZED GLASS BEADS, 5.5-in.-DIA COLUMN

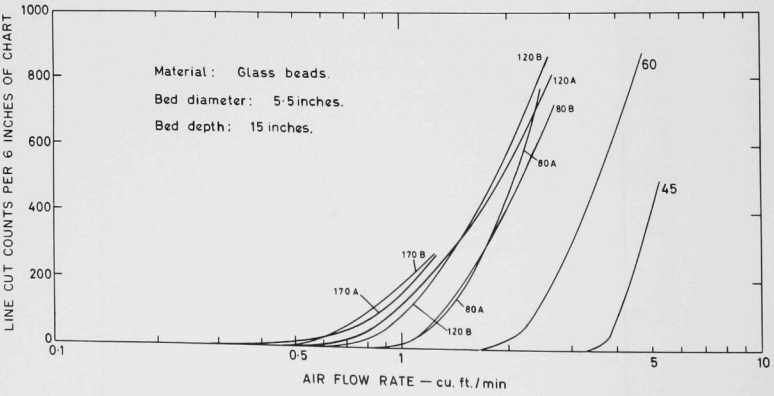

108-7504

Figure 12

INTENSITY MEASUREMENTS AS A FUNCTION OF AIR FLOW RATE FOR VARIOUS-SIZED GLASS BEADS, 11-in.-DIA COLUMN

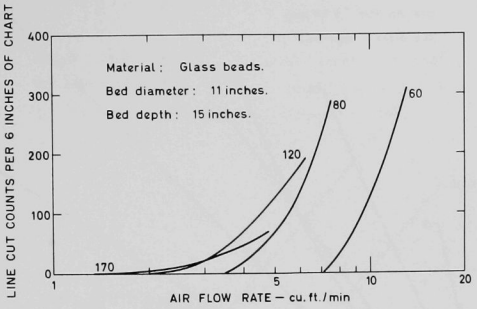

108-7505

Figure 13

INTENSITY MEASUREMENTS AS A FUNCTION OF VELOCITY RATIO FOR VARIOUS-SIZED GLASS BEADS, 3-in.-DIA COLUMN

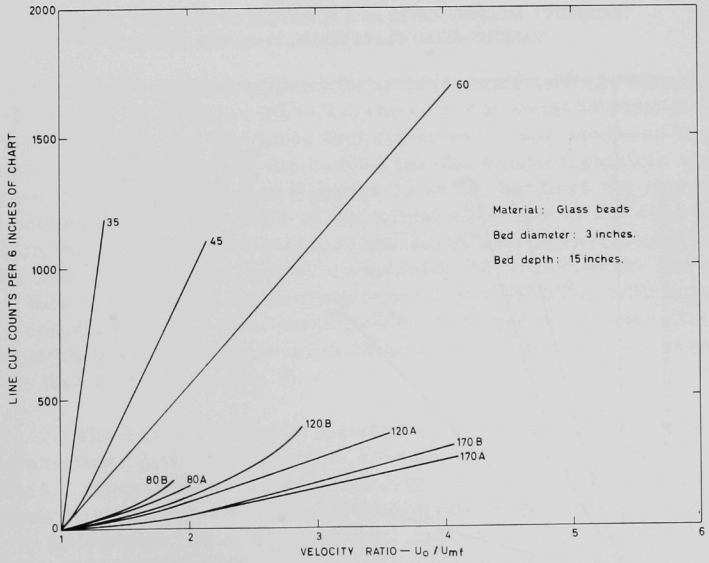

108-7506

Figure 14

INTENSITY MEASUREMENTS AS A FUNCTION OF VELOCITY RATIO FOR VARIOUS-SIZED GLASS BEADS, 5.5-in.-DIA COLUMN

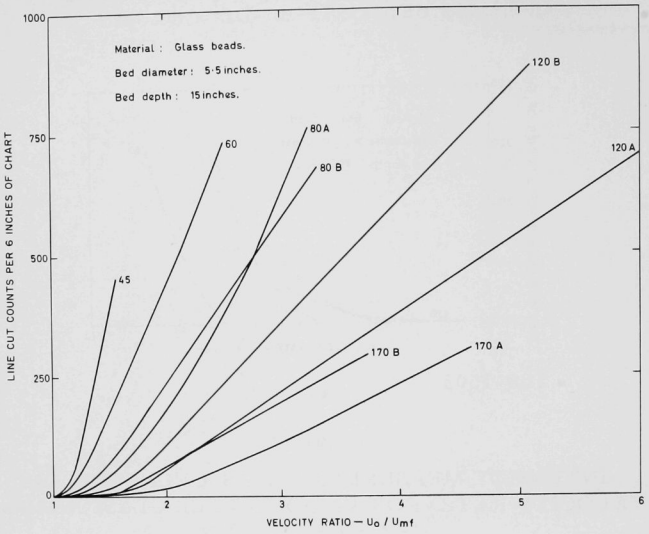

108-7507

Figure 15

INTENSITY MEASUREMENTS AS A FUNCTION OF VELOCITY RATIO FOR VARIOUS-SIZED GLASS BEADS, 11-in.-DIA COLUMN

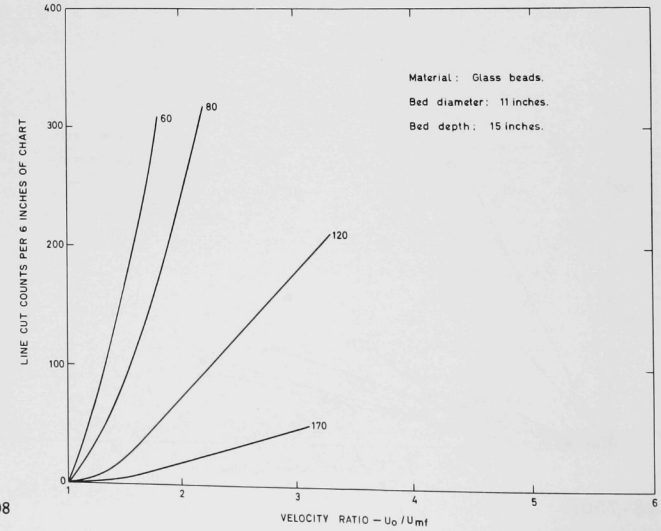

108-7508

Figure 16

INTENSITY MEASUREMENTS AS A FUNCTION OF GAS VELOCITY FOR VARIOUS-SIZED GLASS BEADS

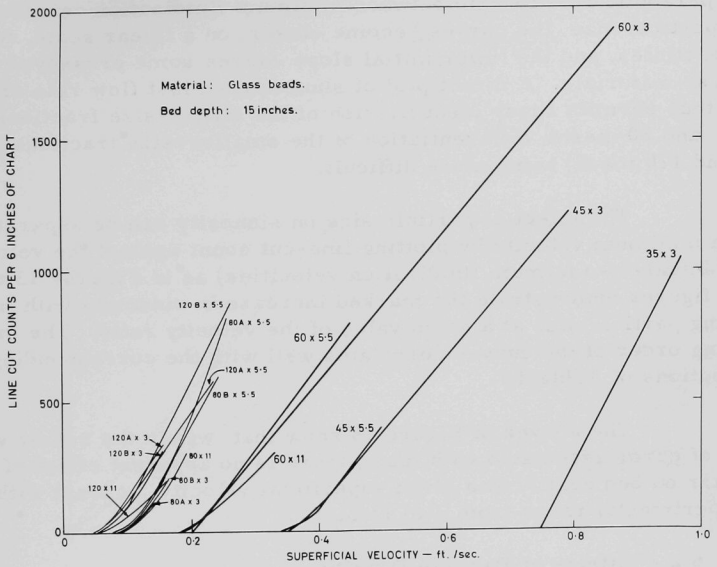

108-7509

All the curves such as those just mentioned are shown in Figures 10 to 16. In Figures 10 to 12, the line-cut count is plotted directly against air flow rate, for the three bed diameters. The abscissa has a logarithmic scale to separate the curves for the smaller particle sizes. The same data are presented in Figures 13 to 15, but here the line-cut count is plotted against the ratio of the actual flow rate to the minimum fluidization value. Figure 16 includes the same data again (except for the 170 mesh data which would further complicate the low-velocity end of the plot), but this time plotted against superficial gas velocity, with data for all three bed diameters on the same graph. In Figures 10 to 16, the data points have been excluded to avoid confusion, the actual scatter being similar to that in Figures 7 to 9.

The results of these experiments substantiate some of the general comments given at the end of Section 3, if trace sinuosity be accepted as a direct measure of bed quality. Thus, Figures 7 to 16 show an increase in sinuosity and hence deterioration in quality, as the gas velocity is increased. Most of the curves appear to be linear, or nearly so, at higher velocities, with a region of increasing slope at the lower end,

this region being dominant in some cases and apparently absent in others. Figure 16 shows that the final slopes for the different materials are approximately the same when plotted in terms of superficial velocity, although the nonlinear portion becomes larger for the smaller particle sizes. Because of the parabolic relationship between minimum fluidization velocity and mean particle size, the curves become closer, on a linear scale, for the finer particles, and the lower initial slope causes some crossover of curves for these materials. A direct plot of sinuosity against flow rate or velocity thus permits ready identification of the larger-size fractions (35, 45, 60, and 80 mesh), differentiation of the smaller-size fractions (80, 120, and 170 mesh) being more difficult.

The effect of particle size on sinuosity can be separated from that on minimum velocity by plotting line-cut count against the velocity ratio (actual-to-minimum fluidization velocities) as in Figures 13 to 15. These figures demonstrate the marked increase in sinuosity with increasing particle size at a given value of the velocity ratio. The increasing order of the curves correlates well with the corresponding size distributions of Table 1.

The curves of Figure 16 show that, within the rather wide limits of error associated with them, there is no apparent effect of bed diameter on bed quality at a given superficial velocity, at least within the experimental range from 3 to 11 in.

6.2.2 Effects of Particle Density

The effect of increased particle density was determined by the use of copper shot instead of glass, the two densities being in the ratio of about 3.6 to 1. The actual size distribution of the copper shot was as follows:

+30 mesh	0.8%
-30 +35 mesh	5.9%
-35 +40 mesh	78.8%
-40 +45 mesh	8.9%
-45 +50 mesh	5.5%
-50 mesh	0.1%
	100.0%

It is therefore reasonable to compare the behavior of this copper shot with that of the "35 mesh" glass beads. This is done in Figure 17, in which the line-cut count is plotted against the velocity ratio for both glass beads and copper shot in the 3-in.-dia bed. Because of the greater pressure drop across the copper shot, the probe spacing was reduced to 3 in. in this case, but retained at 6 in. for the glass beads (the lower probe being 6 in. from the base for both materials).

Figure 17

INTENSITY MEASUREMENTS AS A FUNCTION OF VELOCITY FOR MATERIALS OF DIFFERENT DENSITIES

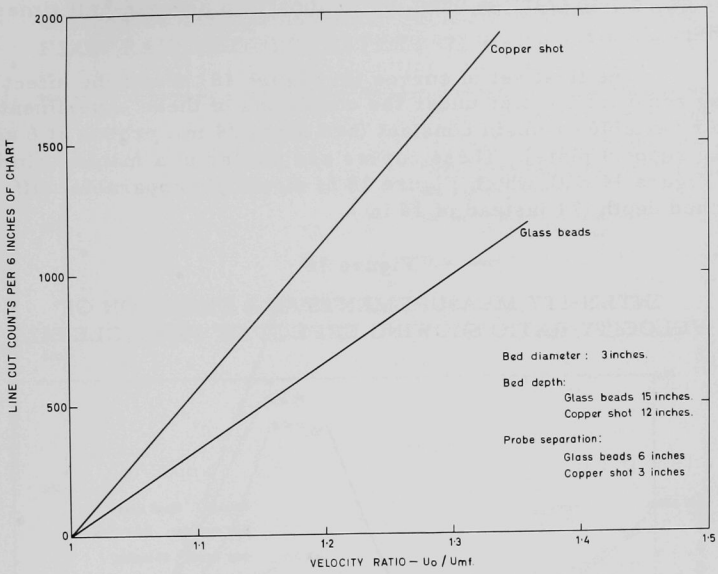

108-7510

The effect of increased particle density is demonstrated by the data from this experiment. If the same probe separation of 6 in. had been used for both materials, the increase in sinuosity with the copper shot would have been even greater. (The effect of probe separation on sinuosity is described in the section immediately below.)

6.2.3 Effects of Bed Height and Probe Position

These experiments were carried out in the $5\frac{1}{2}$-in.-dia tube, using the following values of system variables:

(a) Bed-particle size: 60, 80, 120, and 170 mesh;

(b) Bed depth: 6, 12, 18, 24, and 30 in.;

(c) Lower probe positions: 0, 6, 12, 18, and 24 in. from the support plate, as appropriate to bed depth;

(d) Probe separation: 3, 6, and 9 in., as appropriate to bed depth and lower probe position.

A total of 160 experiments is obtained from all available combinations of these variables. Since it is not practical to present all 160 graphs, typical examples are presented in Figures 18 to 21. The experiments were conducted over a velocity range from the minimum fluidization velocity for the particular size fraction used, up to about one and one-half times the minimum.

The first set of curves (in Figure 18) shows the effect of changing bed-particle size under the conditions of these experiments while the other variables remain constant (bed depth 24 in., probes at 6 and 12 in. from the support plate). These curves are plotted in a manner similar to that of Figure 14 with which Figure 18 is directly comparable, differing only in bed depth (24 instead of 15 in.).

Figure 18

INTENSITY MEASUREMENTS AS A FUNCTION OF VELOCITY RATIO SHOWING EFFECT OF PARTICLE SIZE

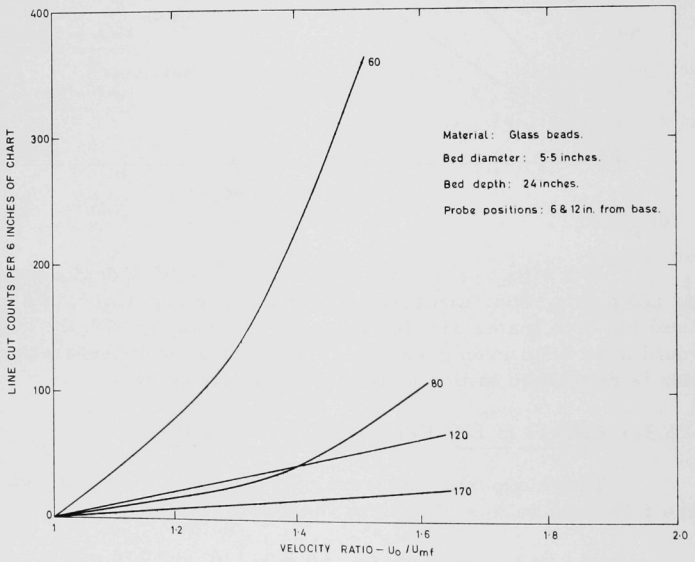

108-7511

The effect of the position of the probes along the bed axis is demonstrated in Figure 19 which includes two sets of curves, one for the 60 mesh material in a 24-in.-deep bed, and the other for the 120 mesh beads in a 30-in. bed. A constant probe separation of 6 in. applies to all the curves. In this case, the curves show the line-cut count plotted against

actual gas flow rate rather than a velocity ratio, for a set of lower probe positions increasing by 6-in. intervals from the support plate.

Figure 19

INTENSITY MEASUREMENTS AS A FUNCTION OF AIR FLOW RATE SHOWING EFFECT OF PROBE POSITION

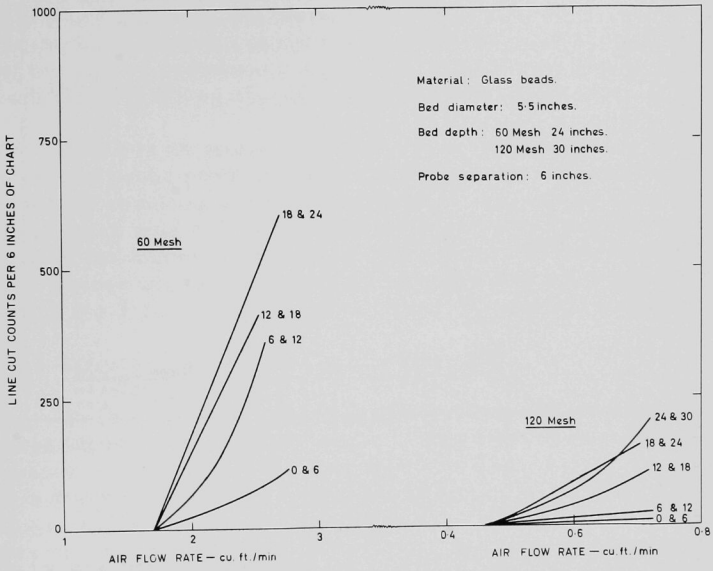

108-7512

For a constant position of the lower probe and constant bed depth, the effect of increasing the probe separation is shown in Figure 20. Here again two sets of curves are given (for 60 and 120 mesh material) with air flow rate as the abscissa. The three curves in each set correspond to the three probe separations, viz., 3, 6, and 9 in.

The effect of increasing bed height on bed quality is illustrated in Figure 21, again by two sets of curves with sinuosity plotted against air flow rate. The first set shows the effect on the lowest 6 in. of the bed as the height is increased from 6 to 24 in., and the second set shows the corresponding effect on the uppermost 6 in., in both cases for 80 mesh material.

Figure 20

INTENSITY MEASUREMENTS AS A FUNCTION OF AIR FLOW RATE SHOWING EFFECT OF PROBE SEPARATION

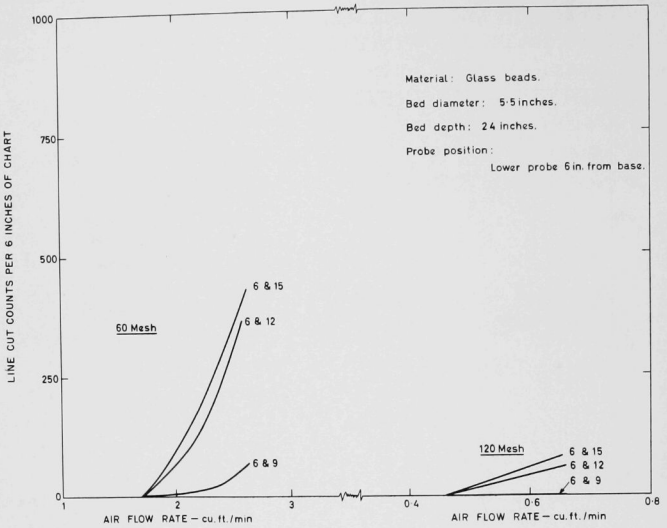

108-7513

Figure 21

INTENSITY MEASUREMENTS AS A FUNCTION OF AIR FLOW RATE SHOWING EFFECT OF BED HEIGHT

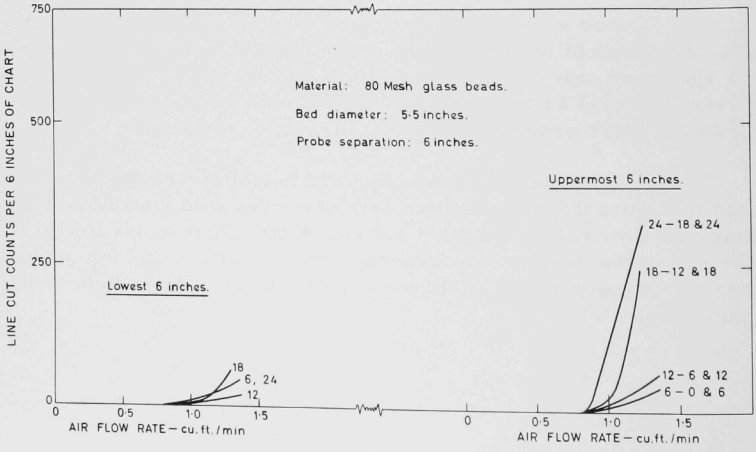

108-7514

These results offer further confirmation of the earlier conclusions on the effects of various bed parameters on bed quality. Thus Figure 19 shows the obvious increase in sinuosity, or decrease in quality, at increasing distance from the distributor, for a constant bed height. As forecast, the sinuosity in a region at a fixed distance from the distributor is not noticeably affected by an increase in the height of bed above that region, as shown in Figure 21, which also shows the increasing sinuosity at the top of a bed as its height increases. These effects of increasing distance from the distributor in decreasing the bed quality must be a combination of the effects of bubble growth, and of increased gas velocity resulting from the decreasing absolute gas pressure up the bed.

There is an interesting effect of increasing probe separation for a given lower probe position, shown in Figure 20. The marked decrease in quality resulting from the increase in separation from 3 to 6 in., and the much smaller change between 6 and 9 in., cannot be explained only by the inclusion of zones further from the distributor and therefore of poorer quality. It may well be related to some natural bubble size, of which the 3-in. separation is too small to take full benefit.

6.2.4 Effects of Particle-size Distribution

To determine the effect of changes in particle-size distribution on bed behavior, tests were made in the 11-in.-dia column with beds composed of mixtures of the size fractions used in previous experiments. One fraction was added to another in known increments (of one or two kilograms) with size analyses made after each addition to follow the changes in size distribution. The starting bed in each case weighed about 32 kg, mixed material being removed after each incremental addition to maintain a constant bed height. The mixtures employed were as follows:

(a) 120 mesh in 1-kg increments added to 60 mesh;

(b) 170 mesh in 1-kg increments added to 80 mesh;

(c) 120 mesh in 2-kg increments added to 170 mesh;

(d) 45 mesh in 2-kg increments added to the mixture of 120 and 170 mesh from (c).

This series of mixtures thus covered the effect of an increasing proportion of fine particles in a bed of coarser ones (a) and (b), of an increasing proportion of coarser particles in a bed of fines (d), and of a gradual change from one fraction to another (c). Abbreviated size analyses of the mixtures are given in Table 2, in which the important changes for each mixture are within the double lines.

Table 2

SIZE ANALYSES OF MIXTURES

Mixture	Size Fraction	Cumulative Additions of Second Component					
		0	1 kg	2 kg	3 kg	4 kg	5 kg
120 mesh into 60 mesh (see Figure 22)	+60	41.1	40.6	38.8	37.1	38.0	37.3
	-60 +100	58.9	56.9	55.9	55.2	51.1	50.4
	-100	0	2.5	5.3	7.7	10.9	12.3
		0	1 kg	2 kg	3 kg	4 kg	5 kg
170 mesh into 80 mesh (see Figure 23)	+80	6.8	6.7	6.5	6.2	5.9	5.4
	-80 +120	91.9	90.5	88.0	86.3	84.5	82.9
	-120	1.3	2.8	5.5	7.5	9.6	11.7
		0	2 kg	4 kg	6 kg	8 kg	10 kg
120 mesh into 170 mesh (see Figure 24)	+120	0	1.8	3.9	5.6	7.7	9.9
	-120 +170	74.1	73.7	71.4	70.6	70.0	69.4
	-170	25.9	24.5	24.7	24.0	22.3	20.7
		0	2 kg	4 kg	6 kg	8 kg	10 kg
45 mesh into combined 170 +120 mesh	+60	0	5.1	9.9	16.7	19.4	26.8
	-60 +100	10.6	10.5	10.1	8.0	7.3	6.6
	-100	89.4	84.4	80.0	75.3	73.3	66.6

Note: Significant size changes for each mixture are within the double lines.

The trace sinuosities for the various mixtures are shown in Figures 22 to 25. In Figures 22 to 24, the sinuosities as determined by line-cut counts are plotted against air flow rate for three of the four mixtures. The air rates used covered the range up to about twice the minimum fluidization value. Under these conditions, the 45 mesh particles added to the (170 + 120) mesh mixture were found to segregate out at the bottom of the bed and to remain unfluidized. Accordingly, the differential pressure traces were unaffected by the addition of the coarse particles, and the line-cut count analyses are not included. The traces that were analyzed in Figure 22 have been reanalyzed in Figure 25 by means of the measurement of actual trace length, which is plotted against air flow rate. The six curves on each of these figures correspond to the original bed material and the mixtures formed by the incremental additions of the other component.

Figure 22

INTENSITY MEASUREMENTS AS A FUNCTION OF AIR FLOW RATE SHOWING EFFECT OF PARTICLE SIZE DISTRIBUTION FOR ADDITION OF 120 MESH TO 60 MESH GLASS BEADS

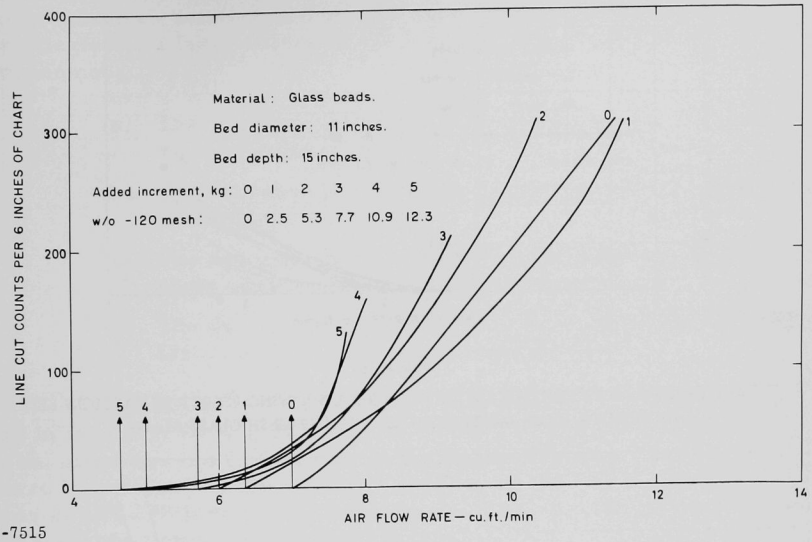

108-7515

Figure 23

INTENSITY MEASUREMENTS AS A FUNCTION OF AIR FLOW RATE SHOWING EFFECT OF PARTICLE SIZE DISTRIBUTION FOR ADDITION OF 170 MESH TO 80 MESH GLASS BEADS

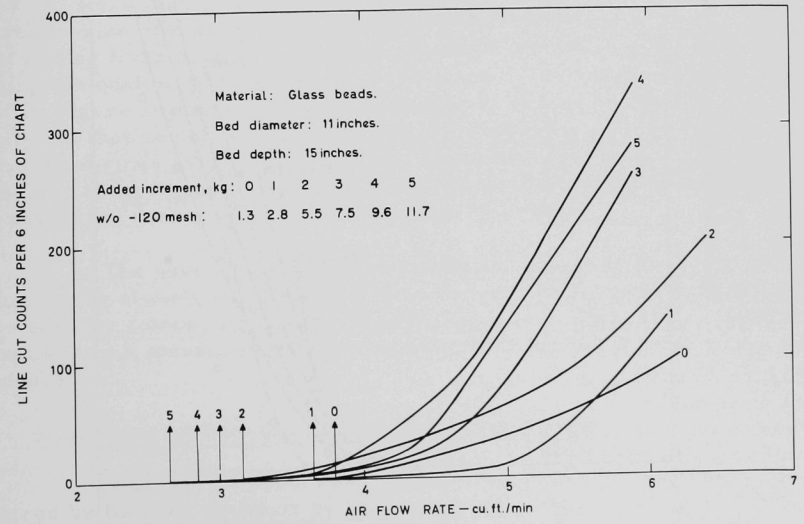

108-7516

Figure 24

INTENSITY MEASUREMENTS AS A FUNCTION OF AIR FLOW RATE SHOWING EFFECT OF PARTICLE SIZE DISTRIBUTION FOR ADDITION OF 120 MESH TO 170 MESH GLASS BEADS

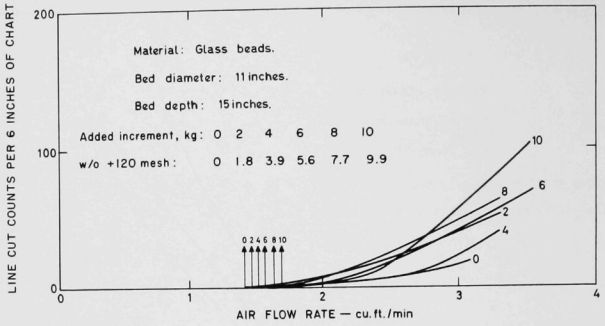

108-7517

Figure 25

TRACE LENGTH AS A FUNCTION OF AIR FLOW RATE SHOWING EFFECT OF PARTICLE SIZE DISTRIBUTION FOR MIXTURE OF 120 WITH 60 MESH GLASS BEADS

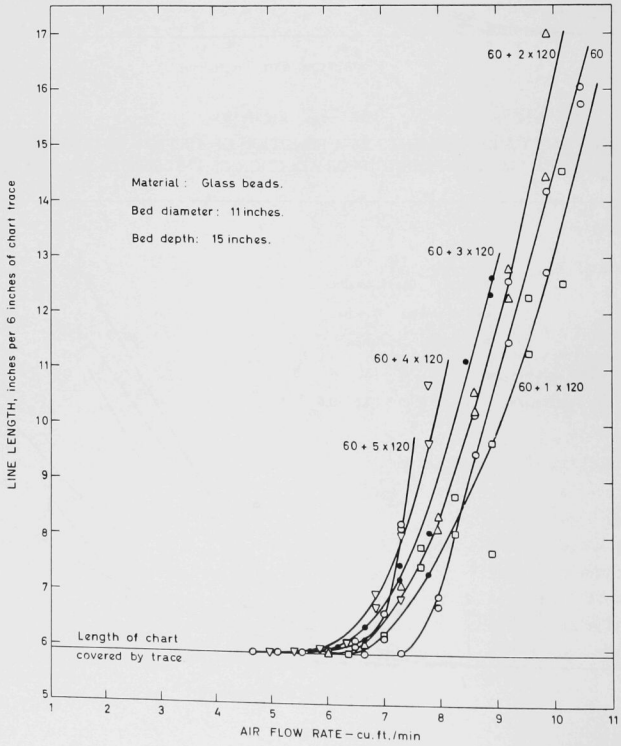

108-7518

The easy distinction between different-sized materials, at least among the larger sizes, afforded by the line-cut count measurements discussed in Section 6.2.1, is borne out to some extent by the data on the made-up mixtures detailed in Table 2. The behavior of these mixtures is complicated to a large extent by the interaction between the following four phenomena:

(a) The decrease in quality with increasing gas velocity or velocity ratio.

(b) The decrease in minimum fluidization velocity with increasing particle size.

(c) The decrease of initial slope of the sinuosity-velocity curve with decreasing particle size.

(d) The decrease in sinuosity with decreasing particle size for a constant value of the velocity ratio.

Operation of the first two of these factors results in an increase in sinuosity for a given velocity as the particle size decreases, while the other two factors operate in the opposite manner, causing a decrease in sinuosity under the same conditions. As can be seen from Figures 22 and 23, the effect of reducing the minimum fluidization velocity proves to be the dominant one, and the result is that, for constant gas velocity, the sinuosity increases as the particle size decreases. This is true both for the addition of 120 mesh to 60 mesh particles (a diameter ratio of 0.55:1), and of 170 mesh to 80 mesh particles (a diameter ratio of 0.60:1). Here then is an important exception to the general conclusions on particle-size effects on bed properties given at the end of Section 3, in that adding finer particles to a bed increases the sinuosity, hence decreasing the quality. The addition of 120 mesh to 170 mesh material, illustrated in Figure 24, results in small changes in minimum fluidization velocity, so that no one of the above factors dominates and the curves present no obvious pattern of behavior. The tendency, as far as there is one, seems to be for an increase in sinuosity with an increase in particle size, compared with a decrease in the other two cases.

The data obtained by measuring the length of the trace reproduced very closely the pattern of the line-cut count measurements, as can be seen by comparing Figure 25 with Figure 22. Thus either method can be used as a measure of trace sinuosity with the same degree of confidence.

6.2.5 General Summary of Particle-size Effects

Although no proof has been offered that trace sinuosity, as measured by line-cut count or by line length, is a direct measure of bed quality, it appears to be a valuable index of the effect of several bed

parameters on the uniformity of fluidization. Of itself, trace sinuosity has proved to be a useful measure of bed-particle size over a fairly wide range. For materials of similar densities, a line-cut count determination could distinguish between average particle sizes in ratios greater than about 1.4. With careful operation, a method employing this technique probably could show a gradual change in particle size or a small increment (in the region of 2 to 5%) of fine particles. It does not seem possible to detect the presence of a small proportion of coarse particles by a technique relying on the response from probes suspended away from the base of the fluidized bed.

Comparatively simple instruments could be developed to measure directly line length (by use of conducting inks) or line-cut counts (by counting the number of passages of a moving arm over a row of point contacts). However, further experimentation concentrating on measurements of trace amplitude and frequency may reveal still closer dependence on bed quality and perhaps more simple instrumentation.

6.3 Behavior of Injected Gas Bubbles

6.3.1 Generated Bubble Size

The volume of air injected into the bed to form a bubble could be determined by calibration of the injection mechanism as described above, coupled with a continual check on the time of opening of the solenoid valve by means of the Visicorder record. However, the bubble produced by an injected burst of air may not have the same volume as that injected. Rowe and Partridge have shown[58] that the ratio of bubble volume to injected volume depends on the fluidization velocity, a ratio of unity being obtained at about 10% above the minimum fluidization velocity.

In the present study, the volume of the injected bubble was determined in the following ways:

(a) By the expansion of the bed following injection, V_e, as measured by the rise in the bed level.

(b) By the apparent volume, V_d, as the bubble burst through the upper surface of the bed, as measured by the apparent diameter, if the bubble was assumed to be spherical.

(c) By the indicated volume, V_c, on the chart records, as measured by the ratio of bubble-trough depth to the average trace level in the absence of bubbles.

These three sets of values, together with the injected volume, V_i, are included in Table 3, each figure in the table being an average of at least 20 measurements. The table also includes the ratios of the three measured bubble volumes to the corresponding injected volume.

Table 3

AVERAGE BUBBLE VOLUMES FOR GLASS BEADS IN A $5\frac{1}{2}$-in.-DIA COLUMN

Solenoid Open Time, sec	Injected Volume V_i, cu in.	Expansion Volume V_e, cu in.	"Observed" Volume V_d, cu in.	"Chart" Volume V_c, cu in.	$\frac{V_e}{V_i}$	$\frac{V_d}{V_i}$	$\frac{V_c}{V_i}$
0.036	2.75	2.95	11.8	13.0	1.07	4.30	4.73
0.088	6.23	5.36	21.9	23.4	0.86	3.52	3.78
0.128	8.91	7.58	35.1	29.9	0.85	3.94	3.36
0.236	13.23	12.66	50.0	37.9	0.96	3.78	2.87

The actual volumes of injected bubbles given in Table 3 vary considerably between the three methods of "measurement." The determination by means of the observed expansion of the total volume of the bed, V_e, must represent the net volume added to the system during injection. Therefore these values agree well with those for the volumes, V_i, injected by the solenoid valve. If it be safe to assume that the degree of expansion of the solid material in the bed is entirely unaffected by the injection of a bubble, then the bubble volume should be equal to that injected. However, the indicated bubble volumes, V_d and V_c, in Table 3 are considerably larger than this.

An explanation for this discrepancy must lie in errors in the measurement of V_d and V_c, or in the assumption that the injected and bubble volumes should be equal. When a bubble reaches the upper surface of a bed, a dome of solid material forms just before the bubble bursts. The diameter of the dome can be as much as twice that of the bubble it encloses, and use of this dome diameter as that of the bubble could lead to bubble volumes up to eight times their actual value. This parameter is clearly one in which little confidence can be placed in absolute terms. However, the dome diameter is useful as an indication of relative size, and is used as such, in Table 4, to show the apparent absence of an effect of bed-particle size on bubble size.

Table 4

OBSERVED BUBBLE DIAMETERS FOR GLASS BEADS IN A $5\frac{1}{2}$-in. DIA COLUMN

Bubble Injection Time, sec	Apparent Bubble Diameter (in inches) at Top of Bed for Given Size of Glass Bead			
	60 Mesh	80 Mesh	120 Mesh	170 Mesh
0.036	2.75	2.75	2.90	2.80
0.088	3.40	3.50	3.45	3.55
0.128	3.90	4.10	4.10	4.00
0.236	4.50	4.65	4.60	4.50

For bubble traces made on the single-pen recorder, the pen would be moving faster for the larger bubbles and the pen inertia error would be greatest for these bubbles. But the data in Table 3 show that the ratio of the volume obtained from the chart measurements to that injected is greatest for the smallest bubbles and considerably less for the largest.

Figure 26

EFFECT OF PROBE-TO-BUBBLE-PATH SEPARATION ON APPARENT BUBBLE VOLUME

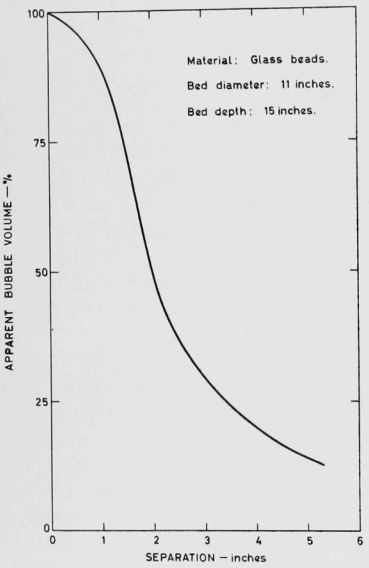

108-7519

The effect of moving the detecting probes horizontally away from the path of the rising bubbles is indicated in Figure 26. This figure shows the proportional reduction in apparent bubble volume as the separation between the probe position and the path followed by the centers of bubbles is increased. The curve is a typical one for the 11-in.-dia bed, but the first section of the curve (up to a separation of about 2 in.) corresponds exactly to the behavior observed in the $5\frac{1}{2}$-in.-dia bed. Thus the error incurred when bubbles do not pass directly up the bed axis cannot be the cause of the bubble-size discrepancy, as this error would never give an indicated volume greater than the true value.

It is quite possible, however, for actual bubble volumes to be greater than the injected volumes, Rowe and Partridge[58] having obtained values of up to twice the injected volume, for superficial velocities about 20% above the minimum fluidization velocity (although their work makes it seem unlikely that a factor of four is possible). Part of the discrepancy can be accounted for in this manner. As it is not out of the question for the whole discrepancy to be so accounted for, the bubble volumes obtained from the single-pen chart records have been used for all the subsequent graphs; i.e., $V_B = V_C$. (The Visicorder traces had too low a signal-to-noise ratio to permit bubble-volume measurements, but bubble-velocity measurements were not affected.)

6.3.2 Effects of Bed-particle Size

Particle size apparently did not affect the volume of bubbles produced in the bed. This is demonstrated by the data of Table 4, which gives the average bubble diameters observed at the top of each bed for the four different injection times and for four different bed-particle sizes.

The average bubble velocities obtained from the various chart records are given in Figures 27 to 30, plotted against the corresponding volumes. Davidson et al.(55) and Harrison et al.(56) demonstrated that bubble velocity (u_B) is proportional to the one-sixth root of the bubble volume (V_B); that is,

$$u_B = kV_B^{1/6}.$$

Curves of the shape represented by the above relationship have been fitted to the data in Figures 27 to 30. The resultant values of k for each bed material have been plotted against the corresponding mean bed-particle size in Figure 31.

Figure 27

BUBBLE VELOCITY AS A FUNCTION OF BUBBLE VOLUME FOR 60 MESH GLASS BEADS

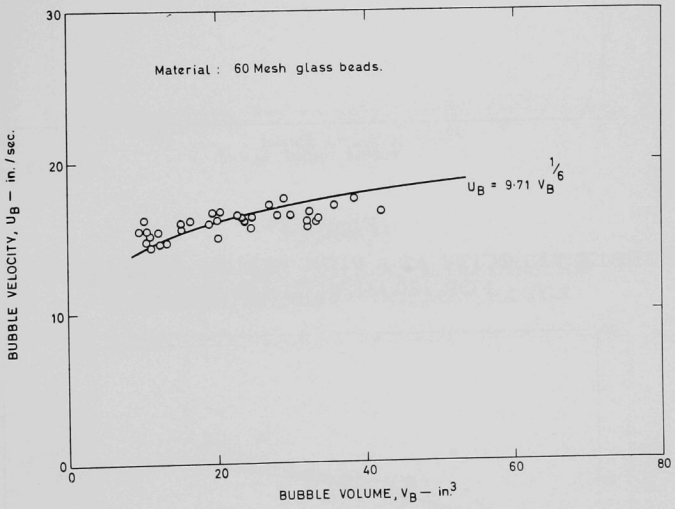

108-7520

The data collated in Figures 27 to 30 show a definite increase in velocity with size of bubble. The curves relating velocity to the one-sixth power of the volume fit the data quite well, the fit being somewhat poorer for the two larger bed sizes. In contradiction to the conclusion of other workers(55,56) that particle size does not affect bubble velocity, these data indicate a dependence on bed-particle size as is shown in Figure 31, the effect being greater for the smaller particle sizes.

Figure 28

BUBBLE VELOCITY AS A FUNCTION OF BUBBLE VOLUME
FOR 80 MESH GLASS BEADS

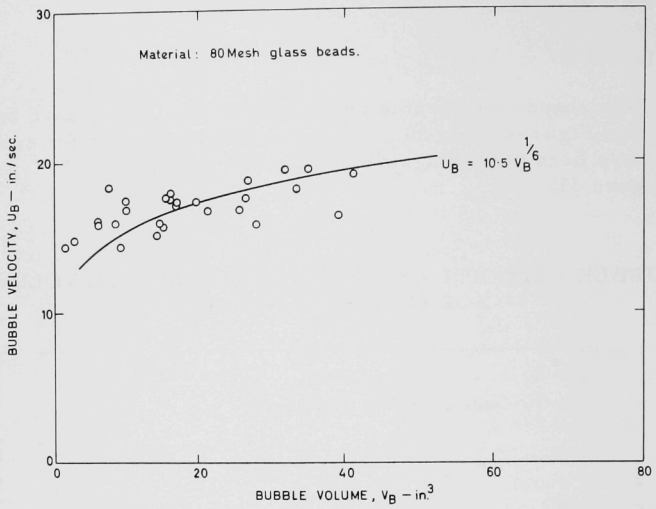

108-7521

Figure 29

BUBBLE VELOCITY AS A FUNCTION OF BUBBLE VOLUME
FOR 120 MESH GLASS BEADS

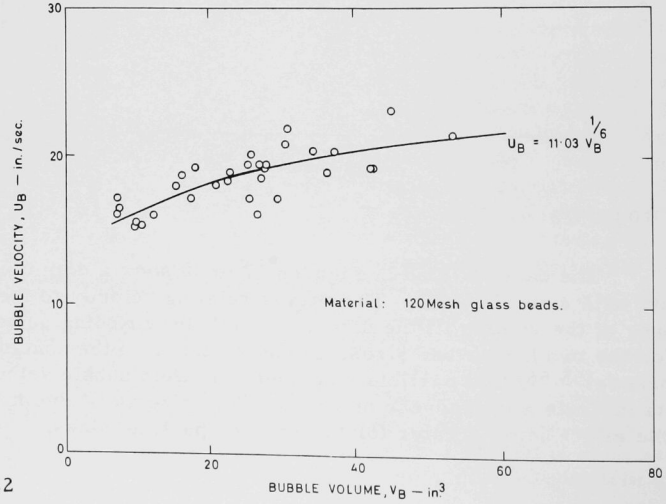

108-7522

Figure 30

BUBBLE VELOCITY AS A FUNCTION OF BUBBLE VOLUME FOR 170 MESH GLASS BEADS

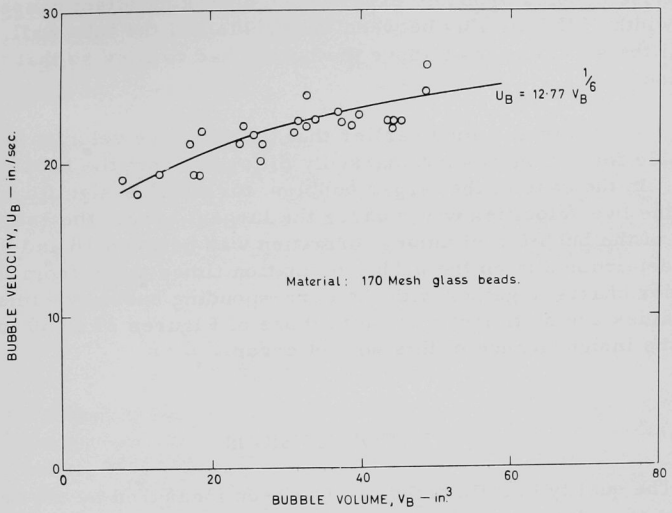

108-7523

Figure 31

EFFECT OF PARTICLE SIZE ON BUBBLE VELOCITY/BUBBLE VOLUME FACTOR

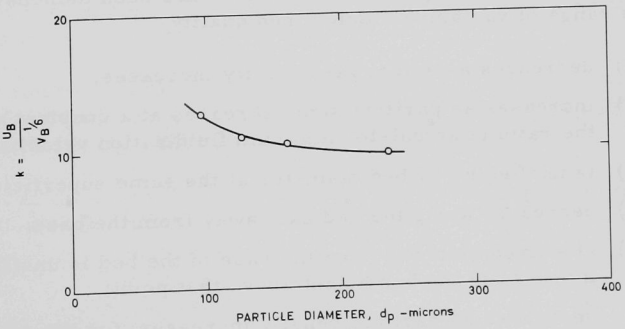

108-7524

Occasionally bubble velocities were calculated that were much less than expected. These almost always corresponded with very large bubbles greater than $4\frac{1}{2}$ in. in diameter. Since the tube diameter was only $5\frac{1}{2}$ in., these bubbles probably experienced a braking effect caused by the narrow width of the annulus between the bubble and the tube wall, through which all the solid material above the bubble had to pass so that the bubble might rise.

It was assumed earlier that the effective velocity associated with bubble formation was not markedly different from the bubble-rise velocity. In the case of the larger bubbles, for which a significant difference in the two velocities would cause the largest error, the average velocity of the bubble roof during formation was between 18 and 30 in./sec, as determined from the bubble formation times taken from the Visicorder charts, together with the corresponding bubble volumes. These values are sufficiently close to those of Figures 27 to 30 to assure the insignificance of this sort of error.

7. CONCLUSIONS

The quality of a fluidized bed has been measured by the degree of sinuosity of a single-pen chart record of the output of a differential pressure transducer connected to two pressure probes on the axis of the bed. The measurement of sinuosity has proved to be a satisfactory method for studying the effects of particle size on some of the properties of the bed.

In agreement with previous studies, it has been demonstrated that within the range of variables studied, bed quality

(a) decreases as actual gas velocity increases;

(b) increases as particle size decreases at a constant value for the ratio of actual-to-minimum fluidization velocities;

(c) is unaffected by bed diameter at the same superficial velocity;

(d) decreases along the bed axis away from the base;

(e) at a fixed distance from the base of the bed is unaffected by an increase in the bed height above that point;

(f) decreases as particle density increases, for the same velocity ratio.

The decrease of minimum fluidization velocity with decreasing mean particle size outweighs the other effects sufficiently to cause a reduction in bed quality as finer particles are added to a fluidized bed, provided that the fines have a mean diameter not much more than half that of the main bed material.

The line-cut count (or line-length measurement) technique applied to a differential pressure-drop trace has proved suitable as a means for observing changes in bed-particle size, and should be easily adaptable to use as a particle-size indication instrument. If operated carefully, such an instrument could indicate a change in average particle size or the increase in fine-particle content, although it does not seem suitable for detecting small increments of coarse particles.

Individual bubble-rise velocities have been shown to increase with increasing bubble size, obeying well enough the law relating velocity to the one-sixth power of the volume. However, in contradiction to earlier assumptions that bubble velocity does not depend on particle size, such a dependence has also been demonstrated, with velocities increasing as particle size decreases.

8. ACKNOWLEDGMENTS

The author's sincere thanks are due to D. J. Raue who carried out much of the experimental work embodied in this report. The author also wishes to acknowledge helpful discussions with N. M. Levitz and A. A. Jonke at Argonne National Laboratory, and Dr. P. N. Rowe at A.E.R.E., Harwell.

9. REFERENCES

1. Morse, R. D., Ind. Eng. Chem., 41, 1117-24 (June 1949).
2. Sutherland, K. S., Trans. I. Chem. E., 39, 188-94 (June 1961).
3. Rowe, P. N., UKAEA Research Group Report, AERE-R 3777, 1961.
4. Rowe, P. H., and Partridge, B. A., UKAEA Research Group Report, AERE-R 3846, 1961.
5. Baron, T., and Mugele, R. A., Unpublished Amer. I. Chem. E. paper (1958).
6. Rice, W. J., and R. H. Wilhelm, A.I.Ch.E. J., 4, 423-9 (Dec 1958).
7. Romero, J. B., Univ. Washington, Ph.D. thesis, 1959.
8. Romero, J. B., and Johanson, L. N., A.I.Ch.E. J., Symposium Ser. No. 38 Fluidization, 28-37 (1962).
9. Bailie, R. C., Fan, L. T., and Stewart, J. J., J. Chem. Eng. Data, 6, 469-73 (June 1961); Ind. Eng. Chem., 53, 567-9 (July 1961).
10. Bartholemew, R. N., and Casagrande, R. M., Ind. Eng. Chem., 49, 428-31 (March 1957).
11. Baumgarten, P. K., and Pigford, R. L., A.I.Ch.E. J., 6, 115-23 (March 1960).
12. Gopichand, T., Sarma, K. J. R., and Rao, M. N., J. Sci. Ind. Res. (India), 168, 97-8 (1957).
13. Grohse, E. W., A.I.Ch.E. J., 1, 358-65 (Sept 1955).
14. Honari, S., Northwestern Univ., Ph.D. thesis, 1958.
15. Schiemann, A., Schuegerl, K., Fetting, F., Roetger, H., Boettger, A., Heidel, K., Merz, M., and Winter, O., Chem. Ing. Tech., 33, 725-38 (Nov 1961).
16. Schuegerl, K., Merz, M., and Fetting, F., Chem. Eng. Sci., 15, 39-74 (July 1961).
17. Stauffer, J. D., Northwestern Univ., Ph.D. thesis, 1956.
18. Yasui, G., and Johanson, L. N., A.I.Ch.E. J., 4, 445-52 (Dec 1958).
19. Daniels, T. C., Rheology of Disperse Systems, 211-21, 1959.
20. Diekman, R., and Forsythe, W. L., Ind. Eng. Chem., 45, 1174-7 (June 1953).
21. Furukawa, J., Ohmae, T., Ind. Eng. Chem., 50, 821-8 (May 1958).
22. Kramers, H., Chem. Eng. Sci., 1, 35-7 (Oct 1951).

23. Liu, F. F. -K., and Orr, C., J. Chem. Eng. Data, 5, 430-2 (Oct 1960).

24. Matheson, G. L., Herbst, W. A., and Holt, P. H., Ind. Eng. Chem., 41, 1099-1104 (June 1949).

25. Peters, K., and Schmidt, A., Oesterr. Chem.-Ztg., 54, 253-8 (1953).

26. Schuegerl, K., Merz, M., and Fetting, F., Chem. Eng. Sci., 15, 75-99 (July 1961).

27. Shuster, W. W., and Haas, F. C., J. Chem. Eng. Data, 5, 525-30 (Oct 1960).

28. Trawinski, H., Chem. Ing. Tech., 25, 229-38 (May 1953).

29. Bakker, P. J., and Heertjes, P. M., Brit. Chem. Eng., 3, 240-6 (May 1958), 4, 524-9 (Oct 1959); Chem. Eng. Sci., 12, 260-71 (July 1960).

30. Dotson, J. M., Chem. Eng. Prog., 54, 188 (May 1958); A.I.Ch.E. J., 5, 169-74 (June 1959).

31. James, F. E., Washington Univ., Ph.D. thesis, 1953.

32. Martin, J., and Andrieu, R., Journée de Fluidisation, 59-67 (1956).

33. Morse, R. D., and Ballou, C. O., Chem. Eng. Prog., 47, 199-204 (April 1951).

34. Brazelton, W. T., Unpublished ANL memo, 1959.

35. Brennecke, L. F., Washington Univ., Ph.D. thesis, 1955.

36. Fitzgerald, T., Unpublished ANL memo, 1960.

37. Henwood, G. A., and Thomas, D. G. A., Instrument Practice, 8, 606-8 (1954).

38. Reboux, P., Journée de Fluidisation, 53-8 (1956).

39. Shuster, W. W., and Kisliak, P., Chem. Eng. Prog., 48, 455-8 (Sept 1952).

40. Takeda, K., Kagaku Kikai, 21, 124-9 (1957).

41. Tyuryaev, I. Ya., Tsailingol'd, A. L., and Builov, A. B., Khim. Prom., No. 5, 356-9 (1961).

42. Volk, W., Johnson, C. A., and Stotler, H. H., Chem. Eng. Prog., 58, 44-7 (March 1962).

43. Gerald, C. F., Chem. Eng. Prog., 47, 483-4 (Sept 1951).

44. Leva, M., Fluidization, 100-107, 1959.

45. Littlewood, G., UKAEA DEG memo, 606(S), 1960.

46. Massimilla, L., and Westwater, J., A.I.Ch.E. J., 6, 134-8 (March 1960).

47. Furukawa, J., and Ohmae, T., J. Chem. Soc. Japan, Ind. Chem. Section, 54, 798-800 (1951).

48. Frye, C. G., Lake, W. C., and Eckstrom, H. C., A.I.Ch.E. J., 4, 403-8 (Dec 1958).

49. Goldman, M., Canjar, L. N., and Beckman, R. B., J. App. Chem., 7, 274-84 (May 1957).

50. Gomezplata, A., and Shuster, W. W., A.I.Ch.E. J., 6, 454-9 (Sept 1960).

51. Johnstone, H. F., Batchelor, J. D., Shen, G. -Y., A.I.Ch.E. J., 1, 318-23 (Sept 1955).

52. Mathis, J. F., and Watson, C. C., A.I.Ch.E. J., 2, 518-24 (Dec 1956).

53. Shen, C. -Y., and Johnstone, H. F., A.I.Ch.E. J., 1, 349-54 (Sept 1955).

54. Levitz, N. M., Unpublished ANL memos, Feb 1960, Jan 1961.

55. Davidson, J. F., Paul, R. C., Smith, M. J. S., and Duxbury, H. A., Trans. I. Chem. E., 37, 323-8 (Dec 1959).

56. Harrison, D., and Leung, L. S., Trans. I. Chem. E., 39, 409-14 (Dec 1961).

57. Rowe, P. N., and Sutherland, K. S., Trans. I. Chem. E., 42, 55-63 (March 1964).

58. Rowe, P. N., and Partridge, B. A., to be published.

59. DallaValle, J. M., Micromeritics, 1948.

60. Herdan, G., Small Particle Statistics, 1960.